



# Not as widespread as thought: Integrative taxonomy reveals cryptic diversity in the Amazonian nurse frog *Allobates tinae* Melo-Sampaio, Oliveira and Prates, 2018 and description of a new species

Albertina Pimentel Lima<sup>1</sup> | Miquéias Ferrão<sup>2,3</sup> | Douglas Lacerda da Silva<sup>4</sup>

<sup>1</sup>Coordenação de Biodiversidade, Instituto Nacional de Pesquisas da Amazônia, Manaus, Amazonas, Brazil

<sup>2</sup>Museum of Comparative Zoology, Harvard University, Cambridge, MA, USA

<sup>3</sup>Programa de Pós-Graduação em Ecologia, Instituto Nacional de Pesquisas da Amazônia, Manaus, Amazonas, Brazil

<sup>4</sup>Programa de Pós-Graduação em Zoologia, Universidade Federal do Amazonas, Manaus, Amazonas, Brazil

## Correspondence

Miquéias Ferrão, Museum of Comparative Zoology, Harvard University, Cambridge, MA, USA.

Email: miqueiasferrao@fas.harvard.com

## Funding information

Fundação de Amparo à Pesquisa do Estado do Amazonas, Grant/Award Number: proc. 653/2009 and proj. 003/2009; Museum of Comparative Zoology, Harvard University; Conselho Nacional de Desenvolvimento Científico e Tecnológico, Grant/Award Number: 154325/2018-0; Coordenação de Aperfeiçoamento de Pessoal de Nível Superior

## Abstract

The small size, low vagility, territoriality, and reproductive mode of some Amazonian frogs undermine the wide geographical distribution assigned to them. Species with these features represent excellent models for testing the existence of cryptic diversity in widely distributed species. The nurse frog *Allobates tinae* has recently been described as widely distributed, occurring in various forest types, as well as on both banks of large rivers. Herein, we gather molecular, morphological, bioacoustics, and egg coloration data in order to investigate whether *A. tinae* actually represents a species complex. The sampling effort focuses on ~1,000 km of landscapes in the Purus–Madeira Interfluve (IPM), where two different forest types predominate. We use barcoding algorithm, cluster analysis, and machine learning to test the specific status currently assigned to *A. tinae*. Results were congruent in showing that the two lineages of *A. tinae* occurring in the IPM represent two different species, which can be distinguished from each other by adult morphology, larvae, advertisement call, and molecular data. The species inhabiting open ombrophilous forests in the southern IPM represents *A. tinae* sensu stricto, while the species that inhabits dense ombrophilous forests in the northern IPM represents a new species. We describe this new species and use egg coloration for the first time in the recent taxonomy of *Allobates* as a diagnostic feature. Additionally, we discuss the importance of egg characteristics on the taxonomy of *Allobates* and possible ecological reasons for differences observed in the egg melanin ratio between *A. tinae* sensu stricto and the new species.

## KEYWORDS

Amazonia, bioacoustics, egg coloration, interfluve purus, Madeira, morphology, tadpoles

Albertina Pimentel Lima and Miquéias Ferrão should be considered joint first author.

Contributing authors: Albertina Pimentel Lima (lima@inpa.gov.br) and Douglas Lacerda da Silva (douglaslacerda1992@gmail.com)

## 1 | INTRODUCTION

Around 20% of the anuran species in the Amazon are distributed in areas larger than 1,600,000 km<sup>2</sup>, and they are considered to be widely distributed (Toledo & Batista, 2012). However, the idea that so many species are widely distributed contradicts behavioral and physiological characteristics (e.g., territorialism, low vagility, parental care) of various anuran groups (Kusano, Maruyama, & Kanenko, 1999; Ovaska, 1992; Ringler, Ursprung, & Hödl, 2009; Rocha, Lima, & Kaefer, 2018). Moreover, the convergence of independent lines of evidence has revealed that many of the species regarded as widely distributed in the Amazonia are actually species complexes with smaller geographic distributions (Caminer et al., 2017; Caminer & Ron, 2014; Ferrão et al., 2016; Fouquet, Cassini, Haddad, Pech, & Rodrigues, 2013; Fouquet et al., 2012; Funk, Caminer, & Ron, 2012; Padiá & De la Riva, 2009; Rivadeneira, Venegas, & Ron, 2018; Rojas et al., 2018).

*Epipedobates* Myers, 1987, was described to accommodate *Prostherapis tricolor* Boulenger, 1899, and the genus *Allobates* Zimmermann and Zimmermann, 1988, was described to allocate *Prostherapis femoralis* (Boulenger, 1884). Posteriorly, Myers et al. (1991) synonymized *Allobates* with *Epipedobates*, being revalidated posteriorly by Clough and Summers (2000). Subsequently, Grant et al. (2006) redelimited the genus *Allobates* and included in it about half of the species previously referred to *Colostethus* Cope, 1875. Since then, the genus *Allobates* has received much attention from taxonomists and it has become one of the Amazonian anuran groups most benefited from the popularization of integrative taxonomy. For several decades, populations of small-sized *Allobates* (snout-vent length below 20 mm) from various localities in the Brazilian Amazonia were mainly attributed to two species: *A. marchesianus* (Melin, 1941) and *A. brunneus* (Cope, 1887). However, the redescription of both species based on data from their type localities (Caldwell, Lima, & Keller, 2002; Lima, Caldwell, & Strüssmann, 2009) made it easier to provide a taxonomic reassessment of populations previously assigned to these taxa. Since then, 13 new species of *Allobates* have been described in the Brazilian Amazonia (Frost, 2019).

Recent taxonomic (e.g., Simões, Rojas, & Lima, 2019), systematic (e.g., Grant et al., 2017), phylogeographic (e.g., Maia, Lima, & Kaefer, 2017), and ecological (e.g., Ferreira, Jehle, Stow, & Lima, 2018) studies have improved our understanding of the diversity and geographic distribution of *Allobates*. It is currently known that most Amazonian *Allobates* species are not widely distributed. The most emblematic example of this pattern may be attributed to *A. femoralis*, long regarded as a pan-Amazonian species. Since the last decade, evidence has been consistent in demonstrating that *A. femoralis* is a complex of cryptic species with smaller geographical distributions (Amézquita et al., 2009; Fouquet et al., 2007; Grant et al., 2006, 2017). The taxonomic status of an *A. femoralis* population from the southern IPM was tested through integrative taxonomy (Simões, Lima, & Farias, 2010; Simões, Lima, Magnusson, Hödl, & Amézquita, 2008), resulting in the description of *Allobates hodli* Simões et al., 2010.

Although the phylogenetic relationships between many *Allobates* species have not been elucidated, the distribution of several closely related species in the Brazilian Amazonia seems to be limited mainly by large rivers (Dias-Terceiro et al., 2015; Kaefer, Tsuji-Nishikido, & Lima, 2012; Moraes, Pavan, & Lima, 2019; Tsuji-Nishikido, Kaefer, Freitas, Menin, & Lima, 2012). However, two pairs of *Allobates* species are known to occur within the same large interfluvium. *Allobates femoralis* and *A. hodli* inhabit the IPM, and their geographical boundaries coincide with the existence of different geomorphological domains (Simões et al., 2008, 2010). On the other hand, *A. crombiei* (Morales, 2002) and *A. carajas* Simões et al., (2019), occur in the interfluvium between the Xingu and Tocantins rivers and their geographical boundaries may be associated to changes in altitude and vegetation, since there are no apparent physical barriers separating these species (Simões et al., 2019). These two examples denote that other types of barriers than rivers (e.g., vegetation, altitude, geomorphology) can hinder the distribution of *Allobates* species.

The geographical distribution of *Allobates tinae* Melo-Sampaio, Oliveira, and Prates, (2018) contradicts the standards known for *Allobates*. According to Melo-Sampaio et al. (2018), this small-sized, territorial, and poorly vagile species is widely distributed in Amazonia, occurring in three large interfluvia (Juruá-Purus, IPM, Madeira-Tapajós) and in various forest types (e.g., lowland dense forest, lowland open forest). The genetic structure in *A. tinae* shown in the phylogeny of Melo-Sampaio et al. (2018) coincides with the existence of large rivers and different forest types. The clade constituted by specimens from the southern IPM was recovered as sister to the clade containing specimens in the Juruá-Purus Interfluvium, while the clade from the northern IPM is sister to the clade Juruá-Purus + southern IPM. Finally, the clade occurring in the east bank of Madeira River is the sister to the clades mentioned above. Due to the phylogeographic structure, as well as to the possibility of cryptic diversity, Melo-Sampaio et al. (2018) conservatively delimited the *A. tinae* type series only with specimens collected in open lowland forests in the southern IPM. The phylogeographic structuring turns *A. tinae* into an excellent system to test the existence of cryptic diversity in species widely distributed in Amazonia.

Testing the existence of cryptic diversity throughout the *A. tinae* distribution might require a massive sampling effort, which could take decades to complete, due to logistical issues. On the other hand, testing for the taxonomic status of specific clades of *A. tinae* could be advantageous from a conservationist viewpoint, as populations of this species may be undergoing intense anthropogenic pressure from deforestation in the IPM (Fearnside & Graça, 2006). In this study, we test the taxonomic status of *A. tinae* with focus on two clades occurring in the IPM: the clade distributed in the (a) northern and (b) southern portions. To do this, we resort to classification and barcoding analysis of species conducted with morphological, bioacoustic, and molecular data. In addition, molecular and bioacoustic data from specimens representing the clade distributed in the east bank of the upper Madeira River were analyzed. Based on the results obtained herein, we formally describe the clade distributed in the northern IPM as a new cryptic species.

## 2 | MATERIAL AND METHODS

### 2.1 | Study area and collection procedures

The study area comprises about 1,000 km of landscapes in the IPM and the east bank of the upper Madeira River, Brazilian Amazonia (Figure 1). The IPM can be informally divided into two major ecoregions. The northern portion of the IPM is characterized by high silt and shallow groundwater soils, and it is covered by dense lowland forest predominantly formed by trees and shrubs of small basal area (Cintra et al., 2013; Ferreira et al., 2018; IBGE, 2012; Schietti et al., 2016). On the other hand, the southern portion of the IPM has predominantly clayish soils, being mainly covered by open lowland forest constituted by trees of larger basal area when compared to the northern portion (Cintra et al., 2013; Ferreira et al., 2018; IBGE, 2012; Schietti et al., 2016). Besides that, the average annual rainfall in the IPM ranges from ~2,100 mm in the southern portion to ~2,800 mm in the northern portion of the interfluvium (Alvares, Stape, Sentelhas, Gonçalves, & Sparovek, 2014).

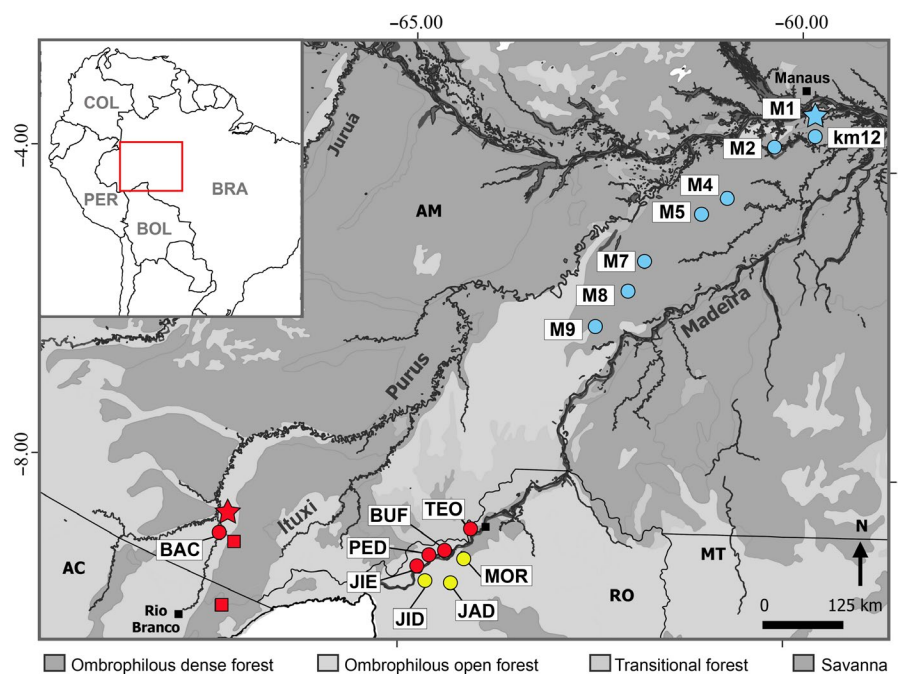
Adult specimens of *Allobates tinae* were sampled between 2009 and 2018 in 13 localities in the IPM, of which 11 represent long-term ecological research modules (hereafter RAPELD; Magnusson et al., 2013): (1) KM12 (−3.46722, −59.81916), (2) RAPELD M1 (−3.371297, −59.864575), (3) RAPELD M2 (−3.683, −60.34), (4) RAPELD M4 (−4.375, −60.957), (5) RAPELD M5 (−4.615, −61.24), (6) RAPELD M7 (−5.246971, −61.963049), (7) RAPELD M8 (−5.647604, −62.162548), (8) RAPELD M9 (−5.957482, −62.489031), (9) RAPELD TEO (−8.828978, −64.075562), (10) RAPELD BUF (−9.133275, −64.497260), (11) RAPELD PED (−9.167074, −64.629109), (12) RAPELD JIE (−9.317073, −64.743354), and (13) BAC (−8.79861, −67.28027)]. The first eight localities are distributed in the northern portion of the IPM, while the others are placed in the southern

portion. The locality BAC is around 5 km far from the *A. tinae*'s type locality (Boca do Acre, Amazonas, Brazil). Three additional localities were sampled in the east bank of the upper Madeira River: (14) RAPELD JID (−9.36194, −64.69194), (15) RAPELD MOR (−9.07611, −64.24611), and RAPELD JAD (−9.46222, −64.39222).

Sixty-eight males and eleven females of *A. tinae* were captured in the IPM, and three males were collected in the east bank of the upper Madeira River. Specimens were killed by overdose of benzocaine topical solution (0.2 mg/g). Muscle tissue samples were collected and stored in absolute ethyl alcohol. Subsequently, the individuals were fixed in 10% formalin and stored in 70% ethanol. Larvae were collected within the territory of a male at RAPELD M1 in March 2017 just after oviposition by an uncollected female and were reared in laboratory until they reached larval developmental stages proper for tadpole description. Tadpoles were killed by overdose of liquid benzocaine and preserved in 5% formalin. Adults and tadpoles were deposited in the herpetological section of the Zoological Collection of the Instituto Nacional de Pesquisas da Amazônia (INPAH), Manaus, Amazonas, Brazil. Specimens were collected under collection permits provided by the Brazilian Institute of the Environment and Renewable Natural Resources (IBAMA) and Chico Mendes Institute for Biodiversity Conservation (ICMBio) (02001.000508/2008-99; 1337-1). Protocols of collection and animal care follow the Biology Federal Council (CFBIO) resolution number 148/2012.

The advertisement calls of seventeen males were recorded in seven localities in the IPM. Nine males were recorded in the northern IPM (two at KM12 and seven at RAPELD M1), and eight males were recorded in the southern IPM (one at RAPELD TEO, BUF, PED, two at RAPELD JIE, and three at BAC). In addition, the advertisement call of two males was recorded in the east bank of the upper Madeira River: one male in the RAPELD JID and one male in the RAPELD JAD. Calls were registered using a ME66 directional microphone

**FIGURE 1** Sampling area in the Purus–Madeira Interfluvium (IPM), Brazilian Amazonia. Outlined red square on the South America map represents the study depicted in the colored map. Blue circles denote sampling sites in the northern IPM. White star shows the type locality of the new species. Red circles represent sampling sites in the southern IPM. Yellow circles denote sampling sites in the east bank of the upper Madeira River (EBMD). Red star shows the type locality of *Allobates tinae* and red squares indicate its paratype localities. Abbreviations: AM = Amazonas, AC = Acre, MT = Mato Grosso, RO = Rondônia



(Sennheiser: Wedemark, Germany) connected to a PMD660 digital recorder (Marantz: Kanagawa, Japan). Air temperature at the moment of recordings was obtained through digital thermohygrometer positioned 1 m above ground.

## 2.2 | Morphology

Sex was determined by secondary sexual characters (e.g., vocal sac and ventral coloration). Maturity of all specimens was determined as adult based on field observation (e.g., calling males, couples in amplexus or females attracted by calling males). Morphometric measurements were taken with a 0.1 mm precision digital caliper or micrometer coupled to a stereoscopic microscope. Twenty-three measurements were made: snout-vent length (SVL); head length (HL); interorbital distance (IO); head width (HW); snout length (SL); eye-nostril distance (EN); internostril distance (IN); eye length (EL); horizontal tympanum diameter (TYM); forearm length (FAL); upper arm length (UAL); thigh length (LL); tibial length (TL); foot length (FL); hand length from the proximal edge of the palmar tubercle to the tip of Finger I (HANDI), tip of Finger II (HANDII), tip of Finger III (HANDIII), and tip of Finger IV (HANDIV); disk width of Finger III (WFD); palmar tubercle diameter (DPT); width of thenar tubercle (WTT); width of Finger III at proximal phalanx (WFP); and width of Toe IV disk (WTD). For hand morphology, we follow Grant et al. (2006). Terminology, diagnostic characters, and measurement definitions followed Caldwell and Lima (2003), Grant et al. (2006), and Lima, Sanchez, and Souza (2007). Description and diagnosis followed Lima, Simões, and Kaefer (2014).

Seventeen morphometric measurements were taken from tadpoles: total length, measured from tail tip to snout tip (TL); body length, measured from snout tip to tail insertion (BL); tail length, measured from tail tip to its insertion into the body (TAL); body width (BW); body height (BH); head width (HWLE); tail muscle width (TMW); maximum tail height (MTH); tail muscle height (TMH); interorbital distance (IOD); internostril distance (IND); eye-nostril distance (END); nostril-snout distance (NSD); eye diameter (ED); vent tube length (VTL); spiracle tube length (STL); and oral disk width (ODW). Developmental stages were determined following Gosner (1960). Terminology, diagnostic features, and measurements followed Altig and McDiarmid (1999) and Schulze, Jansen, and Köhler (2015). Tadpole description followed Schulze et al. (2015).

## 2.3 | Bioacoustics

The advertisement call was characterized as the set of issued notes interspersed by short silent intervals. Spectral parameters were measured by spectrograms generated with a frequency resolution of 82 Hz and 2,048 points, and Blackman window. In order to avoid overlap with background noise, frequencies were measured 20 dB below the peak frequency. The parameters were measured through RAVEN 1.5 (Bioacoustics Research Program, 2015).

Parameters were measured for five calls of each male recorded. We assessed the following parameters: call duration (CD); number of notes (NN); number of pulse per note (NPN); duration of first note (DUR\_N1), central note (DUR\_N2), and last note (DUR\_N3); duration of first silent interval (INT\_1); duration of silent interval after central note (INT\_2); duration of last silent interval (INT\_3); peak frequency of first note (FP\_N1), central note (FP\_N2), and last note (FP\_N3); low frequency of first note (FB\_N1), central note (FB\_N2), and last note (FB\_N3); and high frequency of first note (FA\_N1), central note (FA\_N2), and last note (FA\_N3).

## 2.4 | Sequencing and phylogenetic analysis

Total DNA was extracted from muscle tissue samples of seven specimens from the IPM (four individuals from the northern portion and three individuals from the southern portion) and three specimens from the east bank of the upper Madeira River. Fragments of the 16S ribosomal RNA gene (16S) were amplified by polymerase chain reaction (PCR) by using the 16sar (5'-CGCCTGTTTATCAAAAACAT-3') and 16sbr (5'-CCGGTCTGAACTCAGATCACGT-3') universal primers (Palumbi, 1996). Extractions, PCR reactions, and sequencing were performed according to Maia et al. (2017). Sequences were manually checked and edited through Geneious 5.3.4 (Kearse et al., 2012). The length of amplified 16S sequences in this study ranges from 468 to 538 bp. See Table 1 for voucher, localities, and GenBank accession numbers of specimens sequenced in this study.

For phylogenetic reconstruction purposes, we additionally downloaded from GenBank 83 sequences of the 16S, 41 sequences of the 12S ribosomal RNA gene (12S), 31 sequences of the cytochrome c oxidase subunit I gene (COI), 62 sequences of the cytochrome b gene (CYTB), 12 sequences of the 28S ribosomal RNA gene (28S), 16 sequences of the histone H3 gene (HH3), 15 sequences of the recombination activating gene 1 gene (RAG1), 16 sequences of the rhodopsin gene (RHO), 15 sequences of the seven in absentia gene (SINA), and 13 sequences of the tyrosinase gene (TYR) representing 33 species of *Allobates* and four species used to root the tree [*Anomaloglossus stepheni* (Martins, 1989), *Aromobates nocturnus* Myers, Paolillo-O., & Daly, 1991, *Mannophryne collaris* (Boulenger, 1912), and *Rheobates palmatus* (Werner, 1899)]. Taxa and gene sampling followed Melo-Sampaio et al. (2018). Taxa, vouchers, and GenBank accession number are available in Tables S1–S2.

For each sampled gene, sequences were aligned using the CLUSTAL W algorithm (Thompson, Higgins, & Gibson, 1994) as deployed in the software Bioedit 7.2.5 (Hall, 1999) and manually checked. Alignments were then unified in the software Mesquite 3.04 (Maddison & Maddison, 2015), resulting in a final database consisting of 5,914 base pairs and 93 taxa (Alignment S1). Best-fit nucleotide evolution models and partition schemes were determined through PartitionFinder 2.1.1 (Lanfear, Frandsen, Wright, Senfeld, & Calcott, 2016) using Bayesian inference criteria and the PhyML algorithm (Guindon et al., 2010). The resulted evolution models and partition schemes are shown in Table S3. Phylogenetic relationships

**TABLE 1** Voucher, localities, and 16S GenBank accession numbers of sequenced specimens of *Allobates tinae* complex from Purus–Madeira Interfluve and east banks of the upper Madeira, Brazilian Amazonia

Species	Voucher	Locality	GenBank
<i>A. tinae</i> North IPM	INPH41066	KM12, km 12 of the AM-254, Careiro, Amazonas, Brazil	MT108706
<i>A. tinae</i> North IPM	INPH41064	KM12, km 12 of the AM-254, Careiro, Amazonas, Brazil	MT108705
<i>A. tinae</i> North IPM	APL 18655	RAPELD M1, Careiro, Amazonas, Brazil	MT108707
<i>A. tinae</i> North IPM	INPH41047	RAPELD M1, Careiro, Amazonas, Brazil	MT108708
<i>A. tinae</i> South IPM	INPH41031	RAPELD JIE, Porto Velho, Rondônia, Brazil	MT108710
<i>A. tinae</i> South IPM	APL14601	RAPELD JIE, Porto Velho, Rondônia, Brazil	MT108711
<i>A. tinae</i> South IPM	APL16507	RAPELD TEO, Porto Velho, Rondônia, Brazil	MT108709
<i>A. tinae</i> EBMD	APL14710	RAPELD JID, Porto Velho, Rondônia, Brazil	MT108712
<i>A. tinae</i> EBMD	APL14596	RAPELD JID, Porto Velho, Rondônia, Brazil	MT108713
<i>A. tinae</i> EBMD	APL15877	RAPELD MOR, Porto Velho, Rondônia, Brazil	MT108714

Abbreviations: EBMD, east bank upper Madeira River; IPM, Purus–Madeira Interfluve.

were reconstructed via Bayesian Inference using *MrBayes* 3.2.6 (Ronquist et al., 2012) in the web server *CIPRES* (Miller, Pfeiffer, & Schwartz, 2010). Four independent runs of four Markov chains with 10 million generations each were sampled every 1,000 steps. Parameter stationarity and convergence between runs were checked with *Tracer* 1.7 (Rambaut, Drummond, Xie, Baele, & Suchard, 2018). The consensus phylogenetic tree was summarized in *MrBayes* after discarding 25% of trees as burning. Additionally, uncorrected genetic distance and Kimura-2-Parameters distance (Kimura, 1980) between *A. tinae* clades were calculated for the 16S mitochondrial gene using *MEGA* 6.0 (Tamura, Stecher, Peterson, Filipski, & Kumar, 2013).

## 2.5 | Species delimitation

Barcoding algorithms have been widely applied to molecular data in studies evaluating cryptic diversity in neotropical anurans (e.g., Ferrão et al., 2016; Guarnizo et al., 2015). In this study, we apply the Bayesian implementation of the Poisson Tree Process (bPTP) algorithm (Zhang, Kapli, Pavlidis, & Stamatakis, 2013). The bPTP is a model that focuses on the evolutionary speciation process, considering the process through which evolutionary lineages emerged and identifying lineages compatible with the coalescence process. The bPTP was performed with 400,000 MCMC generations, being sampled every 100 generations and using 20% burning via bPTP server on the web (<https://species.h-its.org/>). A 16S gene tree generated through Bayesian Inference in *MrBayes* 3.2.6 (four independent runs, each one with four Markov chains of 10 million generations, sampled every 1,000 steps; gene tree summarized after 25% of burning) was used as input.

Three distinct methods were used to investigate whether male *Allobates tinae* from the southern and northern IPM clades can be differentiated by morphological and bioacoustic data: (a) RandomForest; (b) discriminant analysis of principal components (DAPC: Jombart, Devillard, & Balloux, 2010); and (c) principal component analysis (PCA) associated with multivariate analysis of variance (MANOVA). Analyses were conducted separately for morphological

and bioacoustic data. To conduct the morphological RandomForest, 23 morphometric measurements were used from 36 adult males of *A. tinae* from the northern IPM clade and 32 males from the southern IPM clade. Bioacoustic RandomForest was conducted with 16 measurements for the advertisement call of 17 males of *A. tinae*, being nine males from the northern IPM clade and 8 males from the southern IPM clade. Each RandomForest was conducted through the construction of 4,000 classification trees. DAPCs were conducted with the same database used to perform RandomForest. The bPTP delimitation was used as input in DAPC. The PCA with bioacoustic data was conducted with the same database used by RandomForest and DAPC, while PCA with morphometric data was conducted with SVL and 22 morphometric ratios (measurements/SVL). The number of retained principal components (PCs) was obtained through the broken stick model, which retained the first 3 PCs for both PCAs. To verify the existence of statistical difference in the morphometric and bioacoustic space occupied by males of *A. tinae* from northern and southern IPM, MANOVAs were conducted using PCs as dependent variables and phylogenetic clades as an independent variable, using  $\alpha = 0.05$ . Data from specimens collected in the east bank of the upper Madeira River were not included in the above cited analysis due to the low number of males and recordings.

Morphological and bioacoustic analyses were conducted on the *R* platform (R Core Team, 2017). The RandomForest algorithm was executed through the package *RandomForest* 4.6-14 (Liaw & Wiener, 2002), and DAPC was executed through the package *Adegenet* 2.1.0 (Jombart & Ahmed, 2011). PCA and MANOVA were executed through the package *Stats* 3.4.1 (R Core Team, 2017).

## 3 | RESULTS

### 3.1 | Phylogenetic relationships

Phylogenetic analysis based on 10 genes recovered *Allobates* as monophyletic (Fig. S1). The clade constituted by *Allobates olfersioides*

from the Atlantic Forest was recovered as sister to *A. undulatus* and all other species of *Allobates*. Despite the high support for phylogenetic relationships of some species pairs (e.g., *A. flaviventris* + *A. magnussoni*, *A. masniger* + *A. nidicola*, *A. tapajos* + *A. gasconi*), overall posterior probabilities of internal nodes were weak. Three large clades with high support were recovered for *Allobates gasconi*, *A. tinae* and *A. trilineatus* (Fig. S1).

With four strongly supported clades, *Allobates tinae* was the most structured species included in our phylogenetic analyses (Figure 2). The clade distributed in the southern IPM (South IPM) consisted of individuals from the west bank of the upper Madeira River (RAPELD TEO and JIE), in addition to the holotype and a paratopotype from Boca do Acre, Amazonas, Brazil (east bank of the Purus River) and an individual from the Ituxí River (tributary of the east bank of the Purus River). The clade with distribution in the northern IPM (North IPM) consisted of individuals collected in KM12 and RAPELD M1. The North IPM clade was grouped as sister to the clade composed of Tefé + South IPM samples. *Allobates tinae* from the east bank of the upper Madeira River (Guajar -Mirim, RAPELD JID and MOR) were inferred as sister to all above mentioned clades.

## 3.2 | Species delimitation

### 3.2.1 | Molecular

The Bayesian implementation of the PTP algorithm delimited each of the four *A. tinae* clades as different species (Figure 2). Genetic distances between *A. tinae* clades were moderately high for the 16S

rRNA gene (Table 2). The K2P genetic distance between the South IPM and the Tef  clade was 4.1%, while the distance between the South and North IPM clades was 3.7%. The clade with the highest pairwise K2P distance values was the EBMD, with K2P values ranging from 4.7% to 5.2%. See Table 2 for uncorrected p-distances.

### 3.2.2 | Morphology

The RandomForest algorithm conducted with morphometric measurements showed high performance in assigning individuals to their respective clades, with only 11.7% of global error rates. The model correctly classified 33 individuals from the North IPM clade and 27 individuals from the South IPM clade. Five individuals from the North IPM clade and three individuals from the South IPM clade were misclassified, representing 13% and 10% of error, respectively. The most significant morphometric measurements in the morphological classification, according to the RandomForest, were as follows: WFD, HANDI, WFP, WTD, and SL.

DAPC conducted with morphometric measurements resulted in high probability of correctness in the assignment of individuals to their respective clades (Figure 3a). All individuals from the North IPM clade were correctly assigned to their clade of origin, except for one specimen from M9 and M2 (Table S4). The odds of success for individuals from this clade were high  $0.95 \pm 0.15\%$  (0.28–1.00). Similarly, all individuals from the South IPM clade were correctly assigned to their respective clade, with high odds of success ( $0.98 \pm 0.06$ ) only one individual wrongly assigned to the North IPM clade. The morphometric measurements with highest contribution values in the

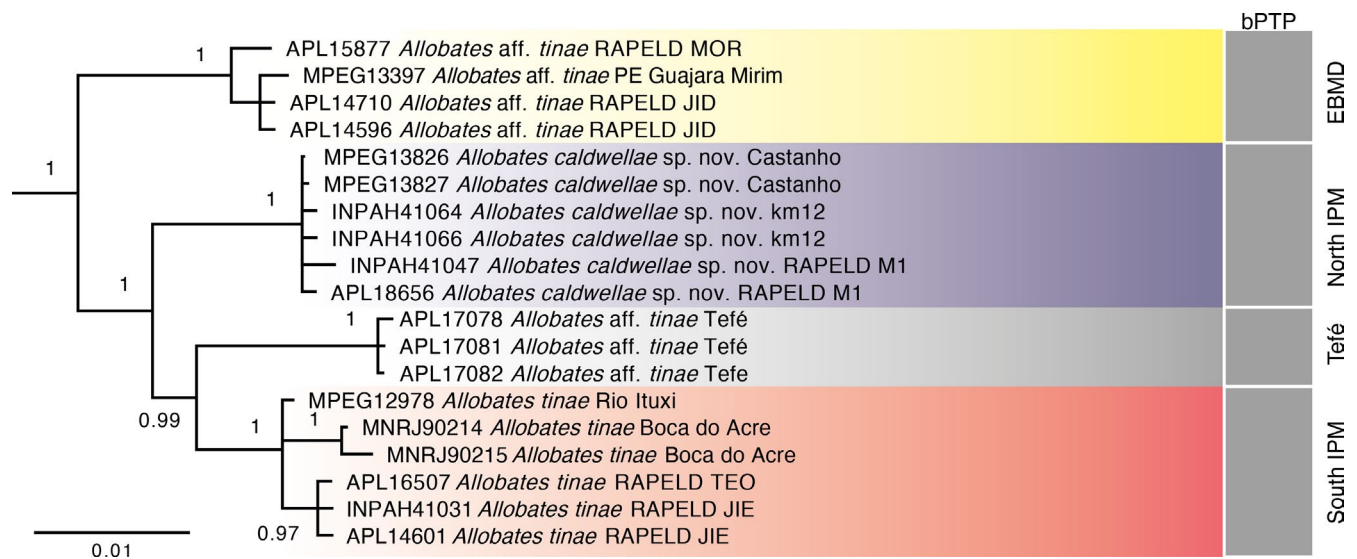


**FIGURE 2** Phylogeny of the *Allobates tinae* species complex based on four mitochondrial (12S, 16S, COI, CYTB) and six nuclear genes (28S, HH3, RAG1, RHO, SINA, TYR). Yellow horizontal bar highlight the clade distributed in the east bank of the upper Madeira River (*A. tinae* sensu lato), blue bar shows the clade distributed in the northern portion of the Purus–Madeira Interfluvium (*A. caldwellae* sp. nov.), gray bar highlight the clade distributed in the municipality of Tef  (*A. tinae* sensu lato), and red bar represents the clade distributed in the southern portion (*A. tinae* sensu stricto). Dark gray vertical bars represent the species delimitation resulted from the Bayesian implementation of the Poison Tree Process. See Figure S1 for the complete *Allobates* phylogeny

**TABLE 2** Pairwise genetic distance (Kimura 2 Parameters = upper diagonal, uncorrected p-distance = lower diagonal) between clades of *Allobates tinae* complex delimited by the Bayesian implementation of the Poisson Tree Process as distinct candidate species. Genetic distance was calculated using the 16S rRNA gene

Clades	1	2	3	4
1 <i>A. tinae</i> EBMD		4.5	5.0	4.6
2 <i>A. tinae</i> South IPM	4.7		4.0	3.5
3 <i>A. tinae</i> Tefé	5.2	4.1		3.5
4 <i>A. tinae</i> North IPM	4.8	3.7	3.7	

Abbreviations: EBMD, east bank upper Madeira River; IPM, Purus-Madeira Interfluve.

DAPC were as follows: WFD, WTD, WTT, HANDII, WFP, and DPT, respectively.

The broken stick model retained the first three PCs of the morphological PCA, which explained together 58.8% of data variation. The multidimensional morphometric space of males from the North IPM clade visually overlapped the space occupied by males from South IPM clade in the first 2 PCs, but little overlap when graphically represented by PC1 + PC3 and PC2 + PC3 (Figure 3b–c). The MANOVA conducted with the first three PCs showed that the two clades of *A. tinae* inhabiting the IPM occupy different multidimensional morphometric spaces (Pillai = 0.56;  $df = 64$ ;  $p = .03$ ). The five morphometric ratios that most contributed to the variation captured by PC1 were as follows: HW, HANDI, TL, HANDIII, and HANDII. However, the most significant variables in PC2 were HANDIV, FAL, TYM, LL, and EL, and in PC3, they were WTD, WFD, WFP, SL, and WTT, respectively (Table 3).

### 3.2.3 | Bioacoustics

The RandomForest algorithm conducted with parameters of male *A. tinae*'s advertisement call showing IPM distribution assigned with absolute accuracy all individuals to their respective clades, where 9 individuals came from the North IPM clade and 8 individuals from the South IPM clade. Temporal parameters were the most significant in correct classification of individuals, where DUR\_N1, DUR\_N2, CD, and DUR\_N3 were the variables that most contributed to correct classification. Just as the RandomForest, DAPC conducted with time and spectral parameters of male advertisement call from the North and South IPM clades assigned individuals to each of their respective clades with 100% hit probability (Figure 3d). However, structural and spectral parameters also contributed to the resulting DAPC classification, in order of importance: NN, INT\_2, FP\_N1, INT\_1, and FA\_N1 (Table S5).

The broken stick model retained the first 3 PCs in PCA with bioacoustic parameters, which explained 85.8% of the data variation (Table 4). The multidimensional bioacoustic space occupied by male *A. tinae* from the South IPM clade does not

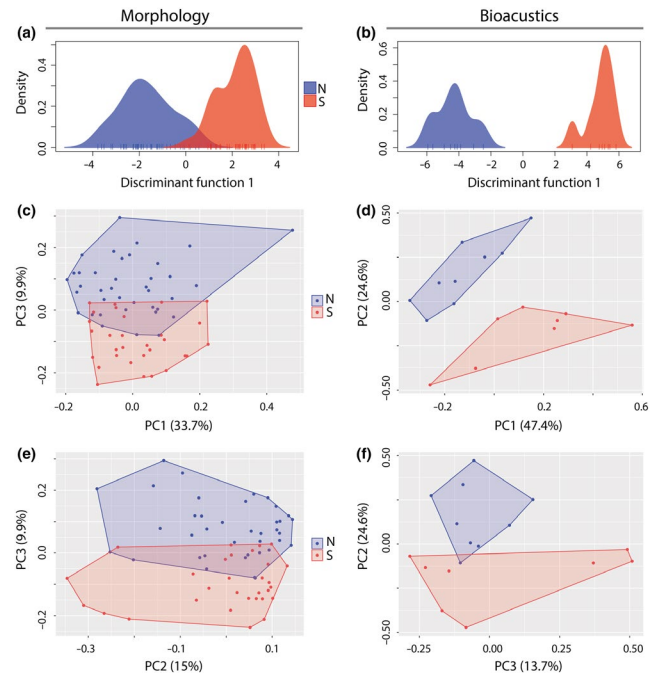


**FIGURE 3** Discriminant Analysis of Principal Components–DAPC (a, d) and Principal Component Analysis–PCA (b–c, e–f) of morphological and bioacoustics data comparing specimens from the northern and southern IPM clades of *Allobates tinae* sensu lato

visually overlap the space occupied by North IPM clade males in PC1 + PC2, slightly overlapping in PC2 + PC3 and overlapping in PC1 + PC3 (Figure 3e–f). The MANOVA including the first 3 PCs as a function of the North and South clades revealed that the advertisement call of males from these 2 clades occupy different multidimensional bioacoustic spaces (Pillai = 0.85;  $df = 14$ ;  $p < .0002$ ). PC1 explained around 47.4% of the data variation, PC2 explained 24.6% of the variation, and PC3 explained 13.7%. The 5 parameters that most contributed in PC1 were as follows: FB\_N3, FP\_N2, FP\_N3, DUR\_N3, and CD. On the other hand, INT\_2, FP\_N1, DUR\_N2, DUR\_N1, and FA\_N1 contributed the most to PC2. The parameters that most contributed to constitute PC3 were INT\_1, FB\_N1, FB\_N2, FA\_N3, and FA\_N3 (Table 4).

Despite not included in the statistical analysis due to the low number of available recordings, the advertisement call of *A. tinae* from the east bank of the upper Madeira River (EBMD) strongly differs from those of males from South and North IPM, and Tefé by having pulsed notes, while the notes emitted by the three latter are clearly unpulsed. Furthermore, the note duration in *A. tinae* EBMD reaches 98 ms, being longer than those emitted by males of the clade Tefé (60 ms), South (79 ms) and North (54 ms) IPM.

### 3.3 | Integrating evidences

The results of analyses used in this study were congruent with each other and showed that specimens of *Allobates tinae* from the South

**TABLE 3** Loadings of SVL and 22 morphometric ratios on the first three principal components generated by a principal component analysis based on 68 males of *Allobates tinae* complex from the northern and southern portion of Purus–Madeira Interfluve, Brazilian Amazonia

Variables	PC1	PC2	PC3	Variables	PC1	PC2	PC3
SVL	0.250	-0.078	0.277	HANDII	-0.263	-0.088	0.010
HL	-0.223	-0.255	-0.125	HANDIII	-0.267	-0.124	-0.220
HW	-0.290	0.025	-0.008	HANDIV	0.023	0.498	0.043
SL	-0.183	-0.160	0.293	WFD	-0.183	0.019	0.403
EN	-0.134	-0.241	0.140	TL	-0.270	0.179	-0.182
IN	-0.211	0.198	-0.083	FL	-0.256	0.196	-0.061
EL	-0.229	-0.269	-0.136	LL	-0.236	0.271	0.025
IO	-0.245	0.093	0.050	DPT	-0.151	0.188	0.162
TYM	-0.117	0.330	-0.072	WTT	-0.046	0.036	0.282
FAL	-0.139	-0.344	-0.232	WTD	-0.149	-0.072	0.437
UAL	-0.256	-0.107	-0.089	WFP	-0.083	-0.150	0.379
HANDI	-0.272	0.075	0.129	Variance (%)	34.17	14.42	10.21

and North IPM clades can be distinguished from each other by molecular, morphological, and bioacoustic data. Based on these results, we describe below the North IPM clade as a new species. Specimens of these two clades also differ from specimens of *A. tinae* EBMD clade by molecular and bioacoustic data. The description of *A. tinae* EBMD clade as a new species is pending additional specimen and tadpole sampling.

## 4 | SYSTEMATICS

### 4.1 | *Allobates caldwella* sp. nov

URN:LSID:ZOOBANK.ORG:ACT:74c9f95c-b689-4242-a0b2-9ab660e84413.

*Allobates* sp. 'Manaus 1' (Grant et al., 2006, p. 299, Fig. 73; Grant et al., 2017, p. 29, Fig. 21).

*Allobates* sp. 'Castanho' (Santos et al., 2009: Fig. S3a; Grant et al., 2017, p. 29, Fig. 21).

*Allobates tinae* (Melo-Sampaio et al., 2018: Figure 3 [clade sp. 'Manaus 1'], Figure 5h).

#### 4.1.1 | Type material

*Holotype* (Figures 4a–c; 5a,c): adult male (INPAH41047) collected by A. P. Lima, on 16 December 2012, in the RAPELD M1 at km 32 of the Brazilian federal highway BR-319 (-3.371297, -59.864575; elevation 50 m a.s.l.), in Careiro, Amazonas, Brazil.

*Paratopotypes* (16 adults): 13 males (INPAH41051, 41052, 41046, 41056, 41049, 41069, 41061, 41057, 41050, 41063, 41067, 41068, 41059) and 3 females (INPAH41045, 41055, 41053) collected by A. P. Lima, E. Salvático, M. M. Silva, D. Lacerda, and N. Melo between February 2011 and March 2018.

*Paratypes* (8 adults): All of them from municipality of Careiro, Amazonas, Brazil. Four males (INPAH41054, 41058, 41066, 41064) collected by A. P. Lima on 7 and 8 November 2009, at km 12 of the

**TABLE 4** Loadings of 16 bioacoustic measurements on the first three principal components generated by a principal component analysis based on the advertisement call of 17 males of *Allobates tinae* complex from the northern and southern portion of Purus–Madeira Interfluve, Brazilian Amazonia

Variables	PC1	PC2	PC3	Variables	PC1	PC2	PC3
CB	0.264	-0.239	0.001	FA_N1	-0.207	-0.290	0.280
DUR_total	0.273	-0.279	-0.082	FP_N2	-0.306	-0.091	0.084
DUR_N1	0.272	-0.296	0.050	FB_N2	-0.269	-0.109	-0.389
DUR_N2	0.269	-0.319	0.019	FA_N2	-0.232	-0.268	0.322
DUR_N3	0.289	-0.273	0.049	FP_N3	-0.292	-0.218	0.120
INT_1	0.049	-0.168	-0.446	FB_N3	-0.307	-0.128	-0.292
INT_2	0.123	-0.384	-0.187	FA_N3	-0.240	-0.225	0.349
FP_N1	-0.219	-0.349	-0.044	-	-	-	-
FB_N1	-0.246	-0.113	-0.436	Variance (%)	47.40	24.64	13.74

Autazes Road (−3.46722, −59.81916); four males (INPAH41062, 41060, 41065, 41048) collected by A. P. Lima on 20 and 21 February 2011, in the RAPELD M2, at km 100 of the Brazilian federal highway BR-319 (−3.683, −60.34).

#### 4.1.2 | Referred material

Seventeen adult males, all of them from state of Amazonas, Brazil: one male (INPAH40970), collected by A. P. Lima on 16 November 2012, in the RAPELD M4, at km 220 of the Brazilian federal highway BR-319 (−4.375, −60.957); five males (INPAH41004, 41011, 40977, 41007, 40969), collected by E. Salvático and M. M. Silva on 31 January 2013, in the RAPELD M5, at km 260 of the BR-319 (−4.615, −61.24); three males (INPAH41008, 40978, 40973) collected by E. Salvático and M. M. Silva on 10 January 2013, in the RAPELD M7, at km 350 of the BR-319 (−5.246971, −61.963049); six males (INPAH41003, 41001, 41005, 40971, 41028, 40975), collected by E. Salvático and M. M. da Silva on 13 and 14 January 2013, in the RAPELD M8, at km 440 of the BR-319 (−5.647604, −62.162548); two males (INPAH41006, 41009), collected by E. Salvático and M.

M. da Silva on 17 January 2013, in the RAPELD M9, at km 450 of the BR-319 (−5.957482, −62.489031).

#### 4.1.3 | Etymology

The specific epithet *caldwellae* honors Dr. Janalee P. Caldwell, the curator emeritus of the Sam Noble Museum of Natural History (Oklahoma, USA), who taught A.P. Lima how to describe *Allobates* and inspired all the authors to work on anuran taxonomy.

#### 4.1.4 | Diagnosis

A medium-sized species of nurse frog allocated in the genus *Allobates* based on phylogenetic relationship and overall external similarity with its congeners. *Allobates caldwellae* sp. nov. is diagnosed by the combination of the following characters: (1) males SVL 14.4–16.9 mm ( $n = 22$ ), females SVL 16.6–16.9 mm ( $n = 3$ ); (2) snout rounded in dorsal and lateral view; (3) in life, adult males and females have brown dorsal surface without hourglass-shaped patterns; presence of dark

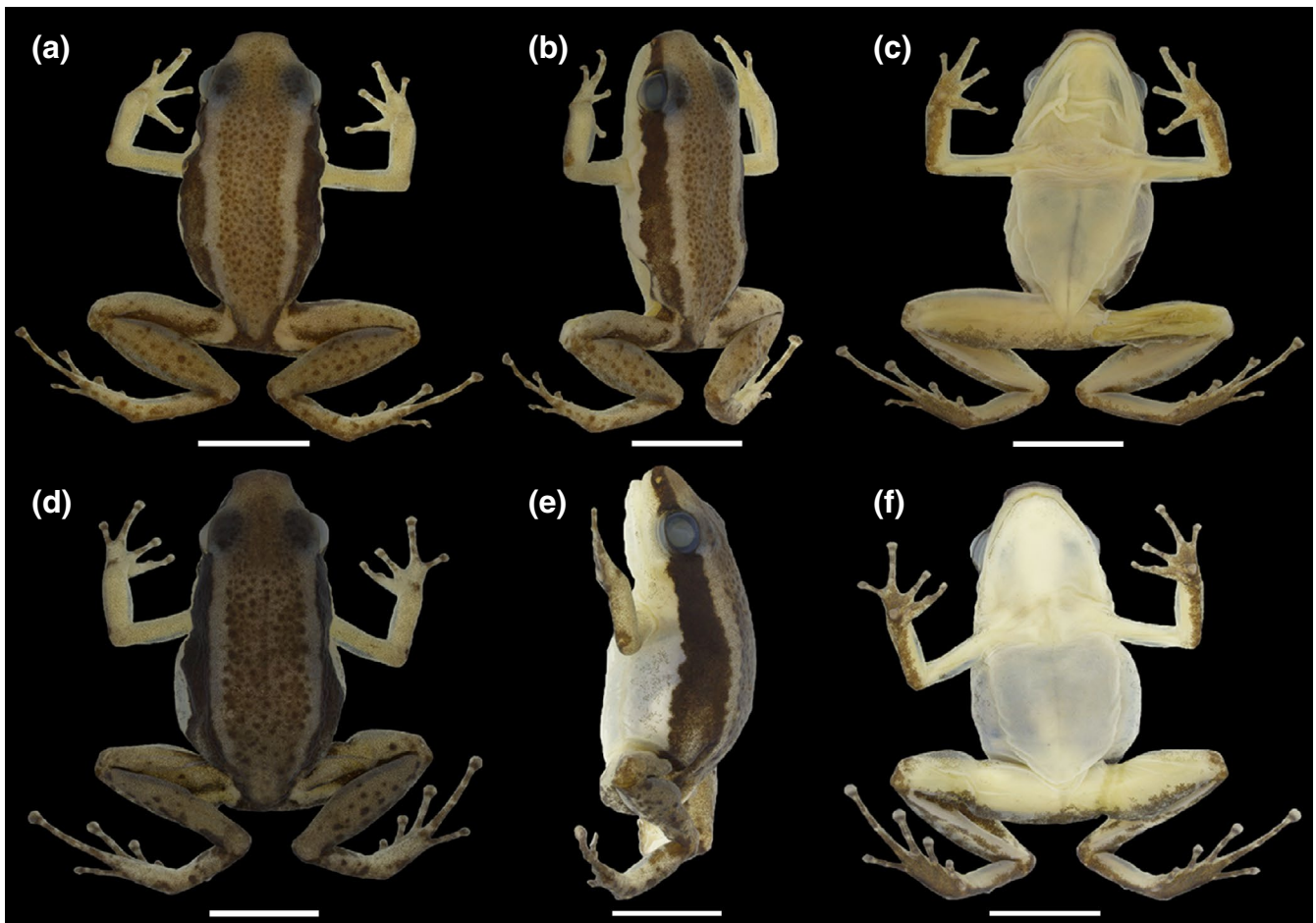


**FIGURE 4** Dorsal, dorsolateral, and ventral views of the adult male holotype INPAH41047 (a–c) and adult female paratopotype INPAH41053 (d–f) of *Allobates caldwellae* sp. nov. from RAPELD M1 sampling site, Careiro, state of Amazonas, Brazil. Scales: 2 mm. Photographs by Jeni Lima Magnusson



**FIGURE 5** Ventral views of the hand and foot of the of the adult male holotype INPAH41047 (a, c) and adult female paratopotype INPAH41053 (b, d) of *Allobates caldwellae* sp. nov. from RAPELD M1 sampling site, Careiro, state of Amazonas, Brazil. Scales: 2 mm. Photographs by Jeni Lima Magnusson

brown granule-shaped pigments on the back, these pigments are delimited by the dorsolateral stripe; (4) presence of conspicuous dorsolateral stripe of light brown color in life and cream color in preservative substance; (5) the dark brown side stripe is well defined, narrow in the nostrils and uniform in width with well-defined edges from the posterior region of the eye sockets; (6) the ventrolateral stripe in life is iridescent white, conspicuous between arm and inguinal region; absent in preserved animals; (7) presence of a pale-colored half-moon shaped paracloacal mark; (8) in life, males have translucent gold yellow chest, throat, and abdomen; melanophores, when present, are concentrated at the edge of the mandible; in preserved material, the chest, throat, and abdomen are cream colored; (9) in life, adult females with throat, thorax, and belly yellowish without melanophores; (10) the iris is golden with black reticulated pattern; (11) single subgular vocal sac; (12) rounded tympanic membrane ranging from 35% to 40% of eye length, partially conspicuous tympanic membrane; (13) paired scutes on all fingers; (14) third phalanx on Finger III of males not swollen, Finger III of males wider than females and of uniform width along all phalanges; (15) Finger III of females of irregular width, basal phalanx wider than the medial and distal phalanges; (16) distal tubercle on Finger IV absent; (17) Finger

II slightly smaller than Finger I and Finger IV; (18) distal phalanx on Finger III around 71% of the disk width on Finger III; (19) the fingertip IV does not reach the distal tubercle on Finger III when juxtaposed; (20) oval thenar tubercle, representing ~54% of the palmar tubercle; (21) metacarpal fold absent; (22) tubercle-shaped, curved, short tarsal keel, not reaching the metatarsal tubercle; (23) basal membrane present between toes III and IV; (24) eggs are laid in a single spawning in clear jelly nests on dead leaves wrapped, folded, or overlapped on the forest floor, and have a dark gray animal pole, covering around 1/2 of the animal hemisphere, a completely whitish vegetal pole; (25) emarginated oral disk in tadpoles; (26) have anterior lip with 3 or 4 short triangular papillae, present on the lateral lip margins, posterior lip entirely surrounded by a row of 12 or 14 triangular papillae, with similar size on the posterolateral and posteromedial margin; (27) adult males vocalize during the day; (28) advertisement calls with an average length of  $771 \text{ ms} \pm 295$  (259–1255 ms) and composed of  $5 \pm 1$  (3–7) notes with an average length of  $41 \text{ ms} \pm 4$  (29–54 ms); average duration of silent interval between notes is  $154 \text{ ms} \pm 31$  (101–216 ms).

#### 4.1.5 | Morphological comparison

We compare the new species with other cryptic-colored species of *Allobates* distributed in lowland forests in Amazonia south of the Amazon River (Appendix 1). Characters of compared species are presented in parenthesis if not otherwise stated. Morphological, bioacoustic, egg coloration, and tadpole comparisons are present separately.

*Allobates caldwellae* sp. nov. differs from *A. carajas*, *A. crombiei*, *A. flaviventris* Melo-Sampaio, Souza, and Peloso, 2013, *A. gasconi* (Morales, 2002), *A. magnussoni* Lima et al., 2014, and *A. tapajos* Lima, Simões, & Kaefer, 2015, by having the dorsum light brown with diminutive dark spots (dark hourglass, rhombus, or “X”-shaped pattern in all species). Males of *A. caldwellae* sp. nov. have golden yellow throat in life (pink to translucent in *A. carajas*; whitish in *A. crombiei*; gray or purplish gray in *A. flaviventris*; gray with black spots in *A. gasconi*; grayish in *A. magnussoni*). Although the color of vocal sac does not distinguish the new species from *A. tapajos*, the new species differs from *A. tapajos* by the absence of dark stripe on thigh and tibia (present in *A. tapajos*).

*Allobates caldwellae* sp. nov. is easily distinguished from *A. bacurau* Simões, 2016, *A. caeruleodactylus* (Lima & Caldwell, 2001), *A. conspicuus* (Morales, 2002), *A. fuscillus* (Morales, 2002), *A. grilisimilis* Simões, Sturaro, Peloso, & Lima, 2013, *A. marchesianus*, *A. masniger* (Morales, 2002), *A. nidicola* (Caldwell & Lima, 2003), *A. nunciatus* Moraes et al., 2019, 2010, *A. subfolionidificans* Lima et al., 2007, *A. trilineatus* (Boulenger, 1884), and *A. vanzolinus* (Morales, 2002) by the vocal sac goldish yellow of males (dark gray, light gray, or grayish in *A. bacurau*, *A. conspicuus*, *A. fuscillus*, *A. marchesianus*, *A. masniger*, *A. nidicola*, *A. nunciatus*, *A. paleovarzensis*, *A. trilineatus*, and *A. vanzolinus*; translucent white

in *A. caeruleodactylus*, *A. grillisimilis*, and *A. subfolionidificans*). Additionally, males of the new species differ from males of *A. bacurau*, *A. fuscillus*, *A. grillisimilis*, *A. masniger*, *A. nidicola*, *A. nunciatus*, *A. paleovarzensis*, *A. trilineatus*, and *A. vanzolinus* by maximum SVL 16.9 mm (maximum SVL 14.7 mm in *A. bacurau*, 17.8 mm in *A. fuscillus*, 15.9 mm in *A. grillisimilis*, 21.5 mm in *A. masniger*, 21 mm in *A. nidicola*, 21.7 mm in *A. nunciatus*, 22.4 mm in *A. paleovarzensis*, 17.2 mm in *A. trilineatus*, and 22.9 mm in *A. vanzolinus*; Morales, 2002; Caldwell & Lima, 2003; Lima et al., 2010; Simões, 2016; Moraes et al., 2019). Although the SVL of males of *A. caldwellae* sp. nov. is similar to that in *A. caeruleodactylus*, *A. conspicuus*, *A. marchesianus*, and *A. subfolionidificans*, the new species differs from *A. conspicuus* and *A. subfolionidificans* by the absence of dark stripe on the thigh and tibia (present in *A. conspicuus* and *A. subfolionidificans*), from *A. marchesianus* by having the head wider than long (longer than wide in *A. marchesianus*), and from *A. caeruleodactylus* by the absence of blue fingers and toe disks (blue fingers and toe disks in *A. caeruleodactylus*).

Although *Allobates caldwellae* sp. nov. is phylogenetically close to *A. tinae*, molecular, morphological, and bioacoustic analyses were congruent in demonstrating that they constitute different species. Even so, we provide below a detailed comparison between these two species. *Allobates caldwellae* sp. nov. differs from *A. tinae* by the yellowish belly in females (translucent white), throat and vocal sac of males without melanophores, or in small numbers only in the portion immediately close to the lower jaw when rarely present (throat and vocal sac with dark melanophores), Finger III in males has a uniform width across all phalanges (basal phalanges wider than medial and distal phalanges), and they have forearm (UAL) longer than arm (FAL) (UAL almost equal to FAL).

#### 4.1.6 | Bioacoustic comparison

The advertisement call of *Allobates caldwellae* sp. nov. (Figure 6a–c) is composed by trills of 3–7 single-notes. This feature distinguishes the call of the new species from the call of *A. bacurau* (60–81 notes: Simões, 2016), *A. caeruleodactylus* (1 note: Lima & Caldwell, 2001), *A. crombiei* (25–59 notes: Lima, Erdtmann, & Amézquita, 2012), *A. flaviventris* (up to 10 notes: Melo-Sampaio et al., 2013), *A. grillisimilis* (1 multipulsed note: Simões, Sturaro, et al., 2013), *A. magnussoni* (1–2 notes: Lima et al., 2014), *A. marchesianus* (21–24 notes: Caldwell et al., 2002), *A. masniger* (1 note: Tsuji-Nishikido et al., 2012), *A. nidicola* (1 note: Tsuji-Nishikido et al., 2012), *A. nunciatus* (up to 10 notes: Moraes et al., 2019), *A. paleovarzensis* (up to 21 notes: Lima et al., 2010), *A. subfolionidificans* (1 note: Lima et al., 2007), and *A. tapajos* (1–2 notes: Lima et al., 2015). *Allobates carajas* issues 4 different types of advertisement call, out of which the most similar in relation to the new species is the type issued in trills; however, *A. caldwellae* sp. nov. trills last from 259–1.255 ms and they are shorter than *A. carajas* trills (up to 22 notes and lasting from 1.49 to 7.05 s: Simões et al., 2019).

*Allobates tinae* sensu stricto is the closest nominal species to *A. caldwellae* sp. nov. Although there is overlap in the spectral parameters regarding the advertisement call of these species, temporal and structural parameters are effective to differentiate them (Figure 6). The advertisement call of *A. caldwellae* sp. nov. (Figure 6a–c) differs from the call of *A. tinae* sensu stricto (Figure 6d–f) by having call duration up to 1.255 s (3.716 s in *A. tinae*: Melo-Sampaio et al., 2018), with no more than seven notes (13 notes in *A. tinae*), and note duration reaching 54 ms (79 ms in *A. tinae*). In addition, the call of *A. caldwellae* sp. nov. is statistically shorter on average  $0.771 \pm 0.296$  s ( $1.85 \pm 0.683$  s in *A. tinae*;  $t = -5.1$ ,  $df = 13.5$ ,  $p = .0001$ ), with fewer notes  $5 \pm 1$  ( $8 \pm 2$  notes in *A. tinae*;  $t = -4.33$ ,  $df = 16.63$ ,  $p = .0004$ ), shorter notes  $41 \pm 4$  ms ( $59 \pm 9$  ms in *A. tinae*;  $t = -8.77$ ,  $df = 11.28$ ,  $p < .0001$ ), and shorter interval between notes  $154 \pm 31$  ms ( $204 \pm 77$  ms in *A. tinae*;  $t = -5.81$ ,  $df = 16.53$ ,  $p < .0001$ ).

#### 4.1.7 | Egg coloration comparison

The freshly laid eggs of *A. caldwellae* sp. nov. (Figure 7a) have dark gray animal pole, covering around 1/2 of the animal hemisphere, with well-defined border and whitish vegetal hemisphere (completely gray animal pole; pigmentation extends to 1/3 of the vegetal pole; inconspicuous edge between poles in *A. tinae* sensu stricto; Figure 7b). Due to the presence of dark gray pigment in the animal hemisphere, freshly laid eggs of *Allobates caldwellae* sp. nov. are distinguished from those of *A. grillisimilis* (light brown animal hemisphere; Figure 7c), *A. subfolionidificans* (white animal hemisphere; Figure 7e), *A. carajas* (white animal hemisphere; Figure 7f), *A. nidicola* (light gray animal hemisphere; Figure 7g), *A. masniger* (light gray animal hemisphere; Figure 7h), *A. flaviventris* (light gray animal hemisphere; Figure 7i), and *A. crombiei* (whitish animal hemisphere; Figure 7j). The jelly where the eggs of *A. caldwellae* sp. nov. are deposited is translucent, and this distinguishes it from the spawning jelly of *A. tapajos* (opaque yellow jelly; Figure 7k), and *A. paleovarzensis* (white and opaque gelatin; Figure 7i). In *A. caldwellae* sp., nov. 1/2 of the animal hemisphere is covered by dark gray pigment, which differentiates the new species from *A. magnussoni* (completely dark gray animal hemisphere; Figure 7d).

#### 4.1.8 | Tadpole comparison

Tadpoles of *A. caldwellae* sp. nov. differ from those of *A. tapajos*, *A. grillisimilis*, *A. caeruleodactylus*, and *A. marchesianus* by having small and triangular labial papillae in the anterior and posterior lips (rounded in the anterior lip and long in the posterior lip in *A. tapajos*; very long in the posterior lip in *A. grillisimilis*, *A. caeruleodactylus*, and *A. marchesianus*). Additionally, they differ from those of *A. caeruleodactylus* and *A. marchesianus* tadpoles by the absence of transverse dark bars at the tail (present in *caeruleodactylus* and *A. marchesianus* tadpoles). *Allobates caldwellae* sp. nov. tadpoles

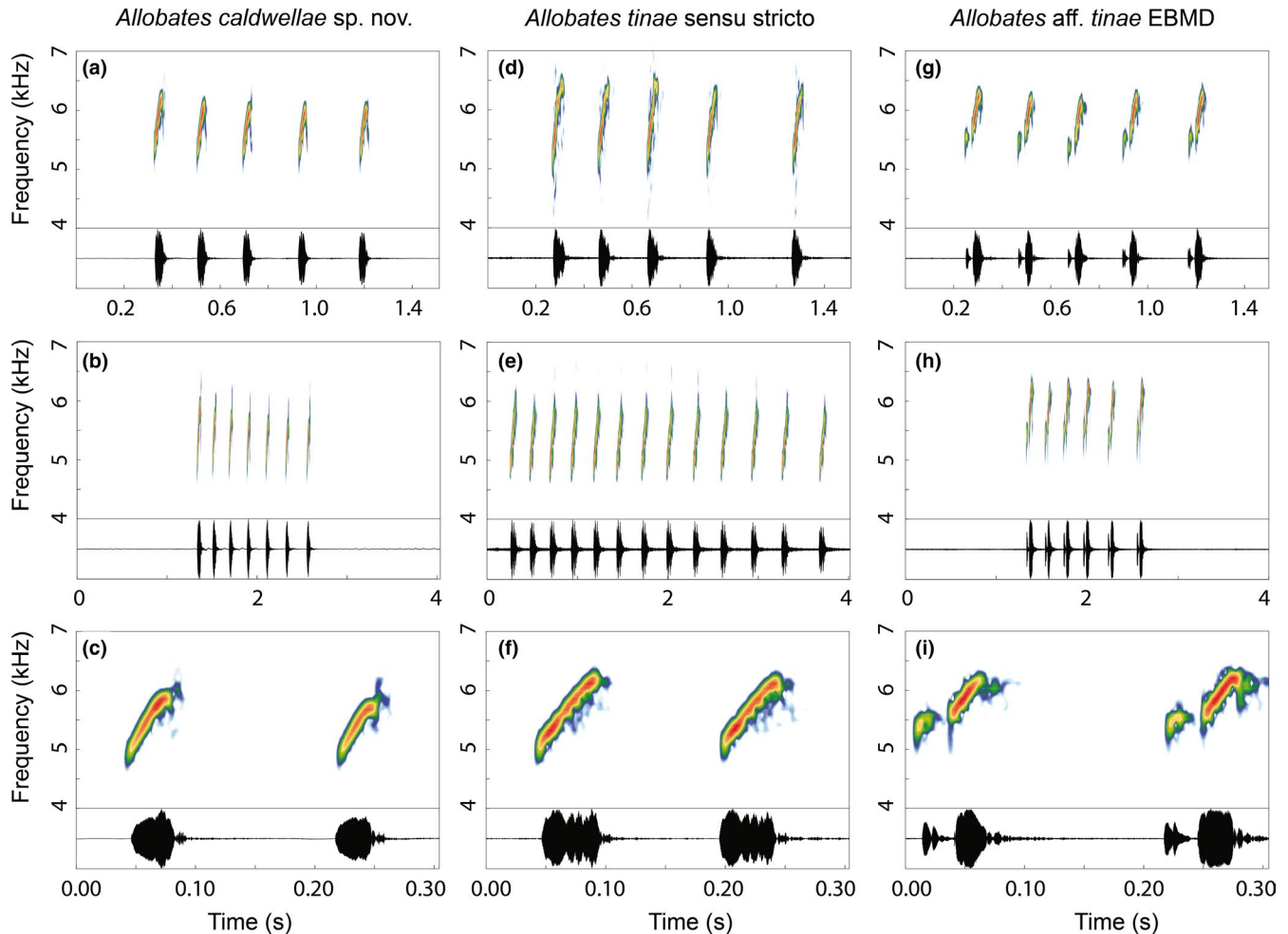


**FIGURE 6** Advertisement call of *Allobates caldwellae* sp. nov. (a–c) from north IPM, *Allobates tinae* sensu stricto (d–f) from South IPM, and *Allobates tinae* sensu lato from the east bank of the upper Madeira River (EBMD). (a, d, g) Calls with five notes. (b, e, h) Calls with the maximum observed number of notes per call in each species. (c, f, i) Detailed views of two notes. (a) INPAH41063, RAPELD M1, Amazonas, SVL = 15.2 mm, temperature = 24.8°C. (b–c) INPAH41068, RAPELD M1, Amazonas, SVL = 16.2 mm, temperature = 24.7°C. (d) Unvouchered, RAPELD JIE, Rondônia, temperature = 25.5°C. (e–f) APL 21678, BAC, Amazonas, SVL = 15.4, temperature = 25.9°C. (g–i) APL16164, RAPELD JAD, Rondônia, temperature = 26°C

differ from *A. paleovarzensis*, *A. magnussoni*, *A. tapajos*, and *A. carajas* tadpoles for having cream colored anteroventral body region in preservative (translucent in all of them: Lima et al., 2010; Lima et al., 2009; Lima et al., 2014; Lima et al., 2015; Simões et al., 2019). They differ from the tadpoles of *A. subfolionidificans*, *A. grillisimilis*, *A. masniger*, *A. nidicola*, *A. paleovarzensis*, and *A. magnussoni* by having at most 4 papillae on either side of the anterior lip and at most 14 papillae in the posterior lip (6 papillae on each side of the anterior lip and 40 in the posterior lip in *A. subfolionidificans*; 5 on each side of the anterior lip; 29 posterior lip papillae in *A. grillisimilis*; absence of papillae in *A. nidicola* and *A. masniger*; 16–19 posterior lip papillae in *A. paleovarzensis*; 12–13 papillae on each side of the anterior lip and 32–35 papillae on the posterior lip in *A. magnussoni*). Additionally, *A. caldwellae* sp. nov. tadpoles differ from *A. nidicola* and *A. masniger* tadpoles by having an aquatic phase (nesting tadpole in *A. nidicola* and *A. masniger*).

#### 4.1.9 | Holotype description

INPAH41047, adult male with SVL 14.7 mm (Figures 4a–c; 5a,c). Body robust, head wider than long (HL represents 84% of the HW); HW/SVL = 0.33 and HL/SVL = 0.28. Snout truncated in dorsal and lateral views; snout length represents 36% of the HW; internostril distance corresponds to 43% of the HW and 53% of the IO; nostrils located posterolaterally to tip of the snout, directed laterally, visible in the lateral and ventral views; internarial region flat. *Canthus rostralis* slightly straight in dorsal view, rounded in cross section. Loreal region slightly flat. Pronounced eye; eye length 0.49 times the HL; eye–nostril distance equal to 70% of the EL. Interorbital region flat; interorbital distance corresponds to 82% of the HW. Tympanum distinct, small and rounded, tympanum diameter represents 35% of the EL; tympanic membrane poorly developed. Tongue attached anteriorly, approximately twice as long as wide (posteriorly), both extremities rounded;



**FIGURE 7** Color of freshly laid eggs of some Amazonian *Allobates*. (a) *A. caldwellae* sp. nov., (b) *A. tinae*, (c) *A. grillisimilis*, (d) *A. magnussoni*, (e) *A. subfolionidificans*, (f) *A. carajas*, (g) *A. nidicola*, (h) *A. masniger*, (i) *A. flaviventris*, (j) *A. crombiei*, (k) *A. tapajos*, (l) *A. paleovarzensis*. Photographs by Albertina Pimentel Lima (a, c–e, g–l), Jesus R. de Souza (b), Pedro Ivo Simões (f)

posterior portion of the tongue twice as wide as the anterior portion; median lingual process absent. Vocal sac single, subgular, covering approximately 2/3 of the subgular region; vocal sac round when inflated. Vocal slits present, extends from the midlateral base of the tongue to the jaw angle, covered anteriorly by the tongue.

Forearm represents 82% of the UAL. Hand small, HANDIII represents 23% of the SVL; relative length of fingers: III > IV > I > II; tip of the Finger IV does not reach the distal tubercle of the Finger III when juxtaposed; phalanges of the Finger III with similar width; Finger III not swollen; distal phalanx width of the Finger III around 78% of disk width on the Finger III; fingers with rounded tips and

dorsal paired scutes present; tips of Fingers III and IV more laterally expanded than on Fingers I and II; lateral fringes and basal membranes between fingers absent; palmar tubercle slightly rounded; palmar tubercle diameter represents 15% of the HANDIII; thenar tubercle width = 0.25 mm wide; one round subarticular tubercle on Fingers I–II and IV; two subarticular tubercles on Finger III; metacarpal fold absent.

Hind limbs robust and long, TL + LL represents 97% of the SVL. Thigh smaller than the tibia (LL/TL = 0.96); tibia length 0.50 times the SVL and thigh length 0.48 times the SVL. Foot length represents 44% of the SVL and 89% of the TL; relative length of

toes IV > III > V > II > I. Presence of one subarticular tubercle on toes I and II; two subarticular tubercles on toes III and V; three subarticular tubercles on Toe IV; proximal subarticular tubercle on Toe IV poorly developed. Supernumerary tubercles absent. Inner metatarsal tubercle longer than wide, raised; outer metatarsal tubercle rounded, raised. Basal membrane present between toes III and IV, absent between the other toes. Tarsal keel present, short and curved, tubercle-shaped, distant from the inner metatarsal tubercle ~1.2 mm. Toe IV disk wider than in Finger III disk (WTD/WFD = 1.2).

Skin granular on the head, upper eyelid and dorsum; dorsal surfaces of the forelimbs smooth; dorsal surfaces of the thigh and tibia smooth with granules scarcely distributed; groin smooth. Skin smooth on the throat, chest, belly and on the ventral surfaces of the forelimbs, tibia and tarsus; ventral surface of thigh areolate.

Morphometric measurements (in mm): SVL, 14.7; HL, 4.1; HW, 4.9; SL, 1.8; EN, 1.4; IN, 2.1; EL, 2.0; IO, 4.0; TYM, 0.7; FAL, 3.0; UAL, 3.7;

HANDI, 2.5; HANDII, 2.4; HANDIII, 3.4; HANDIV, 3.4; WFD, 0.5; TL, 7.3; FL, 6.5; LL, 7.0; DPT, 0.5; WTT, 0.3; WTD, 0.6; and WPF, 0.4.

In preservative, background color of dorsum brownish cream with many dark brown flat granules distributed from snout to the urostyle area; dorsum delimited by a light dorsolateral stripe which extends from the anterior region of the snout to inguinal region. Dark brown lateral stripe presented from the frontal snout to the inguinal region, thinner in the snout area, and thicker from the posterior corner of eyes to the inguinal portion; well delimited from the snout up to 2/3 of the body and lighter close to the groin. Upper part of the tympanum covered by the dark brown lateral stripe, lower part cream. Dorsal surface of arm brownish cream without brown spots. Dorsal surface of hind limbs brownish cream with dark brown spots, without transverse stripes; anterior and posterior thigh dark brown; paracloacal region dark brown. The ventral surface of the throat, legs, and arms cream colored. Belly translucent cream. Ventral surface of the foot and hand cream with several tiny dark brown dots. Color in life is unknown.

**TABLE 5** Morphometric measurements (in mm) of adult males and females of *Allobates caldwella* sp. nov. from northern Purus-Madeira Interfluvio, state of Amazonas, Brazil. Values represent mean  $\pm$  standard deviation (minimum–maximum). See the main text for morphometric abbreviations

Measurements	Type series			Referred specimens	
	Holotype	Males (n = 22)	Females (n = 3)	Males (n = 16)	Female (n = 1)
SVL	14.7	15.6 $\pm$ 0.7 (14.4–16.9)	16.8 $\pm$ 0.2 (16.6–16.9)	14.9 $\pm$ 0.6 (13.2–15.7)	15.7
HL	4.1	4.4 $\pm$ 0.2 (4.0–4.9)	4.4 $\pm$ 0.1 (4.3–4.5)	4.4 $\pm$ 0.3 (3.9–4.9)	4.1
HW	4.9	5.1 $\pm$ 0.1 (4.8–5.4)	5.3 $\pm$ 0.1 (5.2–5.3)	5.1 $\pm$ 0.3 (4.7–5.6)	5.0
SL	1.8	1.8 $\pm$ 0.2 (1.6–2.2)	2.2 $\pm$ 0.0 (2.2–2.2)	2.0 $\pm$ 0.3 (1.5–2.4)	2.1
EN	1.4	1.5 $\pm$ 0.1 (1.2–1.7)	1.5 $\pm$ 0.1 (1.5–1.5)	1.4 $\pm$ 0.1 (1.2–1.6)	1.4
IN	2.1	2.2 $\pm$ 0.1 (2.1–2.3)	2.2 $\pm$ 0.1 (2.2–2.3)	2.1 $\pm$ 0.1 (1.9–2.2)	2.1
EL	2.0	2.1 $\pm$ 0.1 (2.0–2.3)	2.2 $\pm$ 0.0 (2.2–2.2)	2.2 $\pm$ 0.2 (2.0–2.6)	2.1
IO	4.0	4.3 $\pm$ 0.2 (4.0–4.6)	4.5 $\pm$ 0.1 (4.5–4.6)	4.1 $\pm$ 0.1 (4.0–4.4)	4.4
TYM	0.7	0.8 $\pm$ 0.1 (0.7–1.1)	1.0 $\pm$ 0.0 (0.1–1.0)	0.8 $\pm$ 0.1 (0.6–1.0)	0.9
FAL	3.0	3.3 $\pm$ 0.3 (2.9–3.8)	3.4 $\pm$ 0.1 (3.3–3.5)	3.4 $\pm$ 0.3 (2.9–4.0)	3.2
UAL	3.7	3.8 $\pm$ 0.2 (3.5–4.1)	3.9 $\pm$ 0.1 (3.8–4.0)	3.8 $\pm$ 0.3 (3.3–4.2)	3.6
HANDI	2.5	2.7 $\pm$ 0.1 (2.5–3.0)	3.0 $\pm$ 0.1 (2.9–3.0)	2.8 $\pm$ 0.2 (2.4–3.1)	2.7
HANDII	2.4	2.5 $\pm$ 0.1 (2.4–2.8)	2.7 $\pm$ 0.1 (2.7–2.8)	2.5 $\pm$ 0.1 (2.3–2.8)	2.6
HANDIII	3.4	3.5 $\pm$ 0.1 (3.3–3.7)	3.5 $\pm$ 0.1 (3.4–3.6)	3.5 $\pm$ 0.2 (3.2–3.9)	3.4
HANDIV	3.4	3.5 $\pm$ 0.1 (3.3–3.7)	3.5 $\pm$ 0.0 (3.5–3.6)	2.9 $\pm$ 0.5 (2.3–3.6)	3.4
WFD	0.5	0.5 $\pm$ 0.0 (0.5–0.5)	0.6 $\pm$ 0.0 (0.6–0.6)	0.5 $\pm$ 0.0 (0.4–0.6)	0.5
TL	7.3	7.5 $\pm$ 0.3 (6.8–8.0)	7.7 $\pm$ 0.1 (7.6–7.8)	7.4 $\pm$ 0.3 (6.9–8.0)	7.2
FL	6.5	6.6 $\pm$ 0.3 (6.1–7.4)	7.2 $\pm$ 0.2 (7.0–7.3)	6.5 $\pm$ 0.3 (6.0–7.2)	6.7
LL	7.0	7.2 $\pm$ 0.3 (6.7–7.6)	7.5 $\pm$ 0.2 (7.4–7.7)	6.9 $\pm$ 0.3 (6.5–7.4)	7.0
DPT	0.5	0.5 $\pm$ 0.0 (0.5–0.6)	0.5 $\pm$ 0.0 (0.5–0.6)	0.5 $\pm$ 0.1 (0.4–0.6)	0.5
WTT	0.3	0.3 $\pm$ 0.1 (0.2–0.4)	0.3 $\pm$ 0.0 (0.3–0.3)	0.2 $\pm$ 0.0 (0.2–0.3)	0.2
WTD	0.6	0.6 $\pm$ 0.1 (0.5–0.7)	0.6 $\pm$ 0.0 (0.6–0.7)	0.5 $\pm$ 0.1 (0.4–0.7)	0.6
WPF	0.4	0.3 $\pm$ 0.0 (0.3–0.4)	0.3 $\pm$ 0.0 (0.3–0.4)	0.3 $\pm$ 0.0 (0.3–0.5)	0.3

Abbreviation: n, number.

#### 4.1.10 | Variation of the type series

Morphometric measurements are presented in Table 5. The HL represents  $86\% \pm 4$  (71–96) of the HW in males,  $84\% \pm 1$  (83–85) in females; HL  $28\% \pm 1$  (26–31) of the SVL in males,  $26\% \pm 1$  (26–27) in females; SL  $42\% \pm 5$  (36–51) of the HL in males,  $50\% \pm 1$  (49–50) in females; IND  $42\% \pm 1$  (38–45) of the HW in males,  $42\% \pm 1$  (41–42) in females; END  $69\% \pm 6$  (60–79) of the EL in males,  $69\% \pm 2$  (67–70) in females; TYM  $40\% \pm 7$  (31–54) of the EL in males,  $45\% \pm 1$  (44–47) in females. FAL  $88\% \pm 5$  (75–96) of the UAL in males,  $88\% \pm 2$  (86–91) in females; HANDIII  $23\% \pm 1$  (21–25) of the SVL in males,  $21\% \pm 0$  (20–21) in females. Palmar tubercle (DPT)  $14\% \pm 1$  (12–16) of the HANDIII in males,  $15\% \pm 1$  (15–16) in females; WFP  $69\% \pm 8$  (56–80) of the WFD in males,  $58\% \pm 5$  (55–64) in females. TL  $48\% \pm 2$  (45–52) of the SVL in males,  $46\% \pm 0$  (46–47) in females; FL  $43\% \pm 2$  (39–46) of the SVL in males,  $43\% \pm 1$  (42–43) in females. Subarticular tubercles on fingers are similar in size and number to those of the holotype in all individuals.

In life (Figure 8), adult males and females have dorsum light brown, without hourglass-shaped dorsal pattern or large spots; small dark brown granules are distributed on the back in all individuals. All specimens have a light conspicuous dorsolateral stripe beginning at the level of the eyelids and extending to the urostyle region. Dark brown lateral stripe from the tip of snout to the inguinal region, narrow at the tip of snout and relatively uniform width throughout the body; well-defined upper and lower edges.

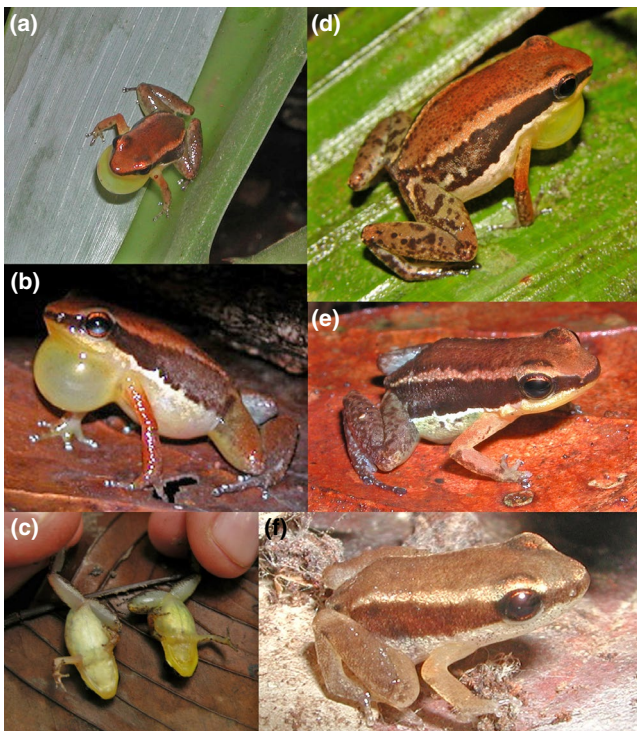


**FIGURE 8** Color in life of *Allobates caldwella* sp. nov. from km 12 of the road to Autazes, Careiro, state of Amazonas, Brazil. Dorsal (a), dorsolateral (b, d–f) and ventral (c) views. Unvouchered specimens

Interrupted, irregular ventrolateral stripe of whitish iridescent color well defined just after the tympanum and diffuse in the middle of the body; in some individuals, it disappears in the inguinal region. Dorsal surface of arms brownish orange. The background color of the dorsal hind limbs brown with dark brown granules; the anterior and posterior region of thighs dark brown; absence of transverse bars on the thigh, tibia, or foot. Light yellow ventral thigh and tibia region is translucent in males, yellowish in females. Pale half-moon shaped paracloacal mark. Throat, vocal sac, and chest goldish yellow in all adult males (Figure 8c) with a few scarce melanophores in the jaw region (except for two individuals with few melanophores on vocal sac), abdomen yellow without melanophores. Adult females with throat, chest, and belly yellowish without melanophores (Figure 8c). Iris golden with black reticulated pattern. The newly metamorphic individual is light brown with a visible pale dorsolateral stripe and brown lateral stripe (Figure 8f).

The coloration in preservative of the type series is similar to that described for the holotype. The variations observed are mainly related to the coloration of the dorsum, which varies from light brown to dark brown. Dark brown granules are present on the dorsum of all individuals, except one male, which has light brown granules. Two males showed melanophores in small concentrations in the central portion of the vocal sac.

#### 4.1.11 | Color of freshly laid eggs and description of tadpoles

Freshly laid eggs of *A. caldwella* sp. nov. have dark gray animal pole, covering around 1/2 of the animal hemisphere; conspicuous edge; whitish equatorial portion. Completely whitish vegetal pole (Figure 7a). Eggs are deposited in translucent jelly.

The description was based on 12 tadpoles in Gosner developmental Stage 36, and measurement values are shown as mean  $\pm$  standard deviation. Maximum and minimum values and morphometric measurements for tadpoles at other stages are shown in Table 6. In dorsal view, the body is ovoid, truncated at the end; triangular in lateral view (Figure 9a–c). Total length (TL)  $21.5 \pm 0.5$  mm; BL  $6.7 \pm 0.1$  mm, BL 31% of the TL; TAL  $14.8 \pm 0.3$  mm, TAL 69% of the TL. Body slightly wider than tall; BH  $2.7 \pm 0.1$  mm, BW  $4.9 \pm 0.2$  mm, BH 54% of the BW; HWLE  $4.5 \pm 0.2$  mm, HWLE 92% of the BW. Rounded snout in lateral and dorsal views; END  $0.7 \pm 0.04$  mm, ED  $1.0 \pm 0.1$  mm, END 75% of the ED. Dorsal eyes, directed dorsolaterally; IOD  $1.2 \pm 0.1$  mm, IOD 26% of the HWLE. Nostrils visible, widely spaced, dorsally located and anteriorly directed; average distance between nostrils is  $1.1 \pm 0.1$  mm. Spiracle centrally located on the left body side, length  $0.6 \pm 0.05$  mm, last third free, opening directed posterodorsally. Vent tube  $1.4 \pm 0.1$  mm, right-sided, long, adhered to the ventral fin. Robust caudal muscle, higher at body insertion ( $2.0 \pm 0.05$  mm), reducing posteriorly ( $1.0 \pm 0.04$  in the middle) up to the tail end ( $0.2 \pm 0.05$ ). Dorsal fin begins at  $4.0 \pm 0.1$  mm after the tail insertion in the body, slightly arched; having almost

**TABLE 6** Morphometric measurements (in mm) of tadpoles of *Allobates caldwellae* sp. nov. from RAPELD M1 at Gosner Stage 33–36, northern Purus–Madeira Interfluve, state of Amazonas, Brazil. Values represent mean  $\pm$  standard deviation (minimum–maximum). See the main text for morphometric abbreviations

	Stage 33 (n = 1)	Stage 34 (n = 2)	Stage 35 (n = 2)	Stage 36 (n = 12)
TL	18.9	18.8–19.4	19.0–19.9	21.5 $\pm$ 0.5 (21.5–22.5)
BL	6.3	5.2–6.4	6.4–6.5	6.7 $\pm$ 0.1 (6.5–7.0)
TAL	12.6	12.6–13	12.6–13.4	14.8 $\pm$ 0.3 (15.5–14.8)
BW	4.3	4.3–4.5	4.4–4.6	4.9 $\pm$ 0.2 (4.6–5.3)
BH	2.5	2.0–2.5	2.5–2.6	2.7 $\pm$ 0.1 (2.6–2.8)
HWLE	3.8	3.8–4.0	4.0–4.2	4.5 $\pm$ 0.2 (4.2–4.9)
TMW	1.6	1.7–1.8	1.8–1.8	2.1 $\pm$ 0.1 (1.9–2.2)
MTH	3.5	3.7–3.9	3.9–3.9	4.1 $\pm$ 0.2 (3.7–4.5)
TMH	1.6	1.7–1.8	1.7–1.8	2.0 $\pm$ 0.1 (1.8–2.2)
IOD	1.0	1.0–1.1	1.0–1.0	1.2 $\pm$ 0.1 (1.1–1.3)
IND	1.0	1.0–1.0	1.0–1.0	1.1 $\pm$ 0.0 (1.0–1.2)
END	0.6	0.7–0.7	0.6–0.7	0.7 $\pm$ 0.0 (0.7–0.8)
NSD	0.4	0.4–0.5	0.4–0.5	0.5 $\pm$ 0.1 (0.4–0.6)
ED	0.8	0.9–0.9	0.9–1.0	1.0 $\pm$ 0.1 (0.9–1.0)
VTL	1.3	1.3–1.3	1.3–1.4	1.4 $\pm$ 0.1 (1.3–1.5)
STL	0.4	0.4–0.4	0.5–0.5	0.6 $\pm$ 0.1 (0.5–0.7)
ODW	1.5	1.5–1.5	1.5–1.6	1.6 $\pm$ 0.1 (1.5–1.7)

Abbreviation: n, number.

uniform width along almost the entire tail ( $1.5 \pm 0.1$  mm in the middle); acuminate tail tip; ventral fin narrower than dorsal fin. It has no flagellum. Lateral line not visible.

Emarginated oral disk, anteroventrally located, average width  $1.6 \text{ mm} \pm 0.1$ . Anterior lip with 3 ( $n = 7$ ) or 4 ( $n = 5$ ) triangular short papillae, separated by a gap of around 1/2 the oral disk width (Figure 9d–e). Posterior lip bordered by a single row containing 12 ( $n = 7$ ) or 14 ( $n = 5$ ) triangular short papillae. Submarginal papillae absent. Upper jaw sheath arch-shaped, lower jaw “V” shaped, both narrow and finely knurled. Dental formula 2(2)/3(1); A-1 measuring  $1.4 \pm 0.1$  mm; A-2 has similar length to A-1, gap of  $0.53 \pm 0.03$  mm. Posterior tooth rows P-1 and P-2 have the same length  $1.36 \pm 0.08$  mm, and row P-3  $1.06 \pm 0.07$  mm.

In preservative, the background color of dorsum, lateral body, and tail muscle cream, covered by dark brown spots of irregular shape and size and formed by aggregated melanophores (Figure 9). The body anteroventral region is light cream colored with dark spots of irregular size and shape; translucent posteroventral body region, allowing intestine visualization. Fins are translucent with whitish reticulation and clustering of melanophores that form irregular dark spots. Color in life is similar to the color in preservative, but the background color of dorsal and lateral surfaces of body is brown.

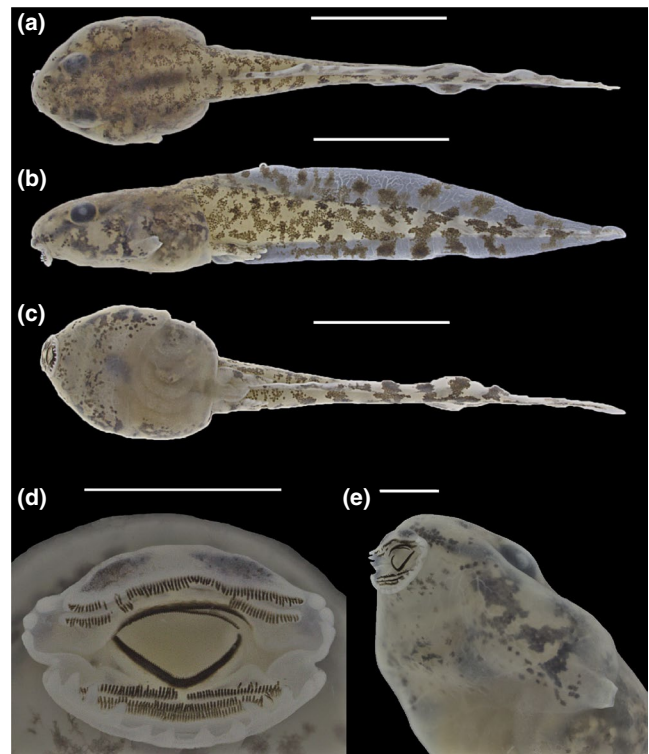


**FIGURE 9** Tadpoles of *Allobates caldwellae* sp. nov. at Gosner Stage 26 from RAPELD M1 sampling site, Careiro, state of Amazonas, Brazil. Dorsal (a), lateral (b) and ventral (c) views of the body. Detailed views of the buccal apparatus (d–e). Scales: a–c, 5 mm; d–e, 1 mm. Photographs by Jeni Lima Magnusson

#### 4.1.12 | Advertisement call

The advertisement call of *A. caldwellae* sp. nov. consists of groups of short tonal notes (trills) with upward modulation (Figure 6a–c). Calls have an average duration of  $777 \text{ ms} \pm 295$  (259–1,255 ms), and they consist of  $5 \pm 1$  (3–7) notes with an average duration of  $41 \text{ ms} \pm 4$  (29–54 ms). The average silent interval between notes is  $154 \text{ ms} \pm 31$  (101–226 ms), being shorter between the first 2 notes [ $124 \text{ ms} \pm 11$  (101–150 ms)] than between the last 2 notes [ $178 \text{ ms} \pm 27$  (122–226 ms)]. Frequencies have similar intensity along the notes in each call: The average dominant frequency is  $5,635 \text{ Hz} \pm 209$  (5,168–6,008 Hz), the lower frequency  $5,387 \text{ Hz} \pm 204$  (4,849–5,817 Hz), and the upper frequency is  $5,829 \text{ Hz} \pm 191$  (5,374–6,206 Hz). Bioacoustic parameters are detailed in Table 7.

#### 4.1.13 | Distribution and natural history

*Allobates caldwellae* sp. nov. is distributed throughout the IPM in the State of Amazonas, Brazil, inhabiting solid ground forest whose phytophysiology is dense ombrophilous forest in the northern IPM (Figure 1). Just as three other *Allobates* species in the region, the reproductive season starts in the beginning of the rainy season, in December (subject to change due to climatic seasonality),

**TABLE 7** Advertisement call of three species of the *Allobates tinae* complex from Brazilian Amazonia. Values represent mean  $\pm$  standard deviation (minimum–maximum). See the main text for bioacoustics measurement abbreviations

	<i>A. caldwellae</i> sp. nov. NIPM (n = 9)	<i>A. tinae</i> stricto sensu SIPM (n = 8)	<i>A. tinae</i> sensu lato EBMD (n = 2)
Temperature (°C)	25.4 $\pm$ 1.2 (24.3–28.5)	25.7 $\pm$ 0.4 (25.0–26.0)	25.5–26.0
NN	4.8 $\pm$ 1.4 (3.0–7.0)	8.0 $\pm$ 2.1 (5.0–13.0)	4.3 $\pm$ 1.4 (3.0–6.0)
NPN	1	1	2
CD (ms)	771 $\pm$ 295 (259–1.255)	1.814 $\pm$ 637 (854–3.485)	977 $\pm$ 270 (705–1.381)
DUR_N1 (ms)	45 $\pm$ 4 (36–54)	63 $\pm$ 8 (48–79)	79 $\pm$ 11 (69–95)
DUR_N2 (ms)	39 $\pm$ 3 (29–45)	58 $\pm$ 8 (45–73)	74 $\pm$ 11 (61–88)
DUR_N3 (ms)	38 $\pm$ 3 (34–49)	56 $\pm$ 9 (42–72)	78 $\pm$ 15 (62–98)
INT_1 (ms)	124 $\pm$ 11 (101–150)	126 $\pm$ 19 (87–0.155)	150 $\pm$ 17 (134–174)
INT_2 (ms)	166 $\pm$ 13 (141–199)	212 $\pm$ 57 (99–414)	172 $\pm$ 23 (153–207)
INT_3 (ms)	178 $\pm$ 27 (122–226)	276 $\pm$ 58 (157–401)	279 $\pm$ 57 (216–412)
FP_N1 (Hz)	5,698 $\pm$ 169 (5,383–6,008)	5,731 $\pm$ 258 (5,125–6,288)	6,007 $\pm$ 168 (5,706–6,201)
FP_N2 (Hz)	5,623 $\pm$ 188 (5,276–6,000)	5,592 $\pm$ 251 (5,125–6,115)	5,888 $\pm$ 94 (5,770–6,093)
FP_N3 (Hz)	5,584 $\pm$ 210 (5,168–5,953)	5,525 $\pm$ 224 (5,060–5,900)	5,950 $\pm$ 127 (5,792–6,137)
FB_N1 (Hz)	5,436 $\pm$ 183 (5,115–5,817)	5,170 $\pm$ 416 (4,583–6,075)	5,119 $\pm$ 158 (4,944–5,377)
FB_N2 (Hz)	5,388 $\pm$ 204 (4,908–5,767)	5,146 $\pm$ 330 (4,596–5,961)	5,184 $\pm$ 130 (4,954–5,346)
FB_N3 (Hz)	5,338 $\pm$ 217 (4,849–5,714)	5,091 $\pm$ 343 (4,618–6,003)	5,203 $\pm$ 166 (5,005–5,387)
FA_N1 (Hz)	5,904 $\pm$ 163 (5,636–6,206)	5,996 $\pm$ 218 (5,626–6,435)	6,253 $\pm$ 74 (6,103–6,326)
FA_N2 (Hz)	5,820 $\pm$ 180 (5,515–6,182)	5,908 $\pm$ 255 (5,509–6,497)	6,200 $\pm$ 65 (6,093–6,295)
FA_N3 (Hz)	5,764 $\pm$ 205 (5,374–6,132)	5,803 $\pm$ 233 (5,356–6,122)	6,225 $\pm$ 45 (6,155–6,298)

Abbreviations: EBMD, East bank of the upper Madeira River; n, number; NIPM, North Purus–Madeira Interfluve; SIPM, South Purus–Madeira Interfluve.

and it finishes in May. Males often vocalize early in the morning, between 5:30 and 9:30 a.m., returning again between 4:00 and 6:30 p.m. They can vocalize all day long under light rain. Males were found vocalizing in leaves on the litter, in small branches, or on vegetation up to 40 cm from the ground. Males attract females to the nests where cephalic amplexus occurs (Figure 10a); after about 5 min, the male leaves the nest (Figure 10b) and the female remains until oviposition (Figure 10c). Eggs are laid in transparent jelly inside rolled, folded, or overlapped leaves on the forest floor (Figure 10d). The spawns are individual, one in each nest. Males take care of spawning and transfer the tadpoles into water (Figure 10e).

## 5 | DISCUSSION

As expected for small-sized species, territorial and poorly vagile (Toledo & Batista, 2012), most of these species have limited geographical distribution. Contrary to the distribution pattern of its congeners and the traces of phylogeographic structuring, *Allobates tinae* has been described as widely distributed in Amazonia (Melo-Sampaio et al., 2018). However, our barcoding and genetic distance (K2P > 3.7%,  $p > 3.5\%$ ) analyses pointed out that the four clades of *Allobates tinae* represented in Melo-Sampaio et al. (2018) and in this study correspond to different species. This finding was corroborated

by the results of morphological and bioacoustic analyses concerning *A. tinae* specimens from two of these clades, one distributed south of the IPM (*A. tinae* stricto sensu) and the other in the northern IPM. The advertisement call of *A. tinae* from the east bank of upper Madeira River also supports the delimitation of this clade as distinct from *A. tinae* sensu stricto. We described herein the northern IPM clade as a new species: *Allobates caldwellae*. Although morphological and bioacoustic data for the *A. tinae* Tefé clade were not evaluated in this study, it should be addressed as candidate species by implication so that *A. tinae* does not remain paraphyletic.

*Allobates caldwellae* and *A. tinae* sensu stricto (only *A. tinae* hereinafter) occur along the IPM, the first being distributed in dense solid ground of ombrophilous forests in the northern IPM, while the other occurs in open ombrophilous forests with palm trees in the southern IPM. Similarly, Ortiz, Lima, and Werneck (2018) found different candidate species of the treefrog *Osteocephalus taurinus* (Steindachner, 1862) inhabiting different types of forests in the IPM. The authors suggest that differences in the IPM forest type might have produced distinct ecological responses in continuous populations of *O. taurinus*, resulting in genetic differentiation. In addition to *O. taurinus*, a newly described tree frog species belonging to the genus *Scinax* has genetic and phenotypic clines (Ferrão et al., 2016, 2017) that coincide with the IPM forest types. Although this study has not been designed to answer evolutionary questions, differences in egg pigmentation in *A. caldwellae* and *A. tinae* may provide clues on ecological adaptation.



**FIGURE 10** Breeding behavior of *Allobates caldwellae* sp. nov. at km 12 of the road to municipality of Autazes, Careiro, state of Amazonas, Brazil. (a) cephalic amplexus, (b) male beside the breeding site after amplexus, (c) female inside the breeding site, (d) freshly laid eggs, (e) male caring the tadpoles on its back

*Allobates caldwellae* eggs deposited in dense forests with low penetration of solar radiation are less pigmented than eggs of *A. tinae* deposited in more open forests and with higher internal solar radiation. The amount of melanin in the eggs of these species may be an outcome of adaptation to solar radiation, which in intense amounts may cause mortality and abnormal embryo development (Blaustein, Kiesecker, Chivers, & Anthony, 1997; Gurdon, 1960). Supporting the radiation-melanin hypothesis in Amazonian *Allobates*, the white eggs of *A. subfo-lionidificans* of open ombrophilous forests are protected from sunlight by being deposited on the undersides of leaves. However, testing the relationship between egg pigmentation and protection from solar radiation in Amazonian *Allobates* still lacks experimentation.

Egg pigmentation in anurans has been used in phylogenetic reconstructions or to diagnose species or genus (Glaw & Vences, 2006; Grant et al., 2006; Ohler & Dubois, 2006; Pinheiro et al., 2019; Sá et al., 2014). In this study, egg pigmentation has proven to be an effective differentiating feature between *A. caldwellae* and other species of *Allobates*. As far as we know, this has been the first time that egg coloration was used to differentiate two *Allobates* species. Although it has shown to be useful for interspecific differentiation, egg coloration in *Allobates* has historically been described with poor detail in species descriptions, being mainly characterized as pigmented (e.g., *A. granti*; *A. magnussoni*) or unpigmented (e.g., *A. subfo-lionidificans*; *A. carajas*). We recommend that further descriptions of *Allobates* species describe and illustrate major features of freshly laid

eggs, such as presence or absence of pigmentation, pigmentation intensity (e.g., black; gray; grayish; light brown), and pigmentation extent (e.g., 1/2 of pigmented animal pole; the whole animal pole; and 1/3 of pigmented vegetal pole), as well as characterization of the boundary between the pigmented and unpigmented portions (e.g., conspicuous; inconspicuous).

#### ACKNOWLEDGEMENTS

This study was funded by PRONEX-FAPEAM/CNPq (proj. 003/2009, proc. 653/2009). Many people helped us in the sampling, and we are thankful to all of them; however, we would like to especially thank to Rafael de Frafa, Marison Prestes, Pedro Ivo Simões, Igor L. Kaefer, Jussara Dayrell, Philip Gleeson (Phill), João Souza (Joãozinho), Moises Mello (Neneco), Pinduca, Eveline Salvático, Guilherme Rezende, and Rubico for their assistance. Santo Antônio Energia S.A. for supporting the fieldwork on the upper Madeira river; Centro de Estudos Integrados da Biodiversidade Amazônica (CENBAM) for assistance with fieldwork at the northern Purus-Madeira Interfluve; Fernanda Werneck and Ariane Silva for access to the INPA-H zoological collection. The holotype and tadpole photographs were taken with equipment acquired under a grant from PRONEX-FAPEAM (ed. 016/2006, proc. 1437/2007) provided to José Albertino Rafael. Miquéias Ferrão received postdoctoral fellowship from CNPq (PDJ process 154325/2018-0) and an Edward O. Wilson Biodiversity Postdoctoral Fellowship from Museum of Comparative Zoology, Harvard University. Douglas Lacerda da Silva received fellowship from Coordenação de Aperfeiçoamento de Pessoal de Nível Superior (CAPES). Specimens were collected under IBAMA/ICMBio permits (02001.000508/2008-99; 1337-1). The funders had no role in study design, data collection and analysis, decision to publish, or preparation of the manuscript.

#### CONFLICT OF INTEREST

The authors declare that they do not have any conflict of interest concerning this manuscript.

#### ORCID

Albertina Pimentel Lima  <https://orcid.org/0000-0003-4586-5633>

[org/0000-0003-4586-5633](https://orcid.org/0000-0003-4586-5633)

Miquéias Ferrão  <https://orcid.org/0000-0001-7035-8276>

#### REFERENCES

- Altig, R., & McDiarmid, R. W. (1999). Body plan: Development and morphology. In R. W. McDiarmid, & R. Altig (Eds.), *Tadpoles: The biology of anuran larvae* (pp. 24–51). Chicago, IL: University of Chicago Press.
- Alvares, C. A., Stape, J. L., Sentelhas, P. C., Gonçalves, J. L. M., & Sparovek, G. (2014). Köppen's climate classification map for Brazil. *Meteorologische Zeitschrift*, 22, 711–728. <https://doi.org/10.1127/0941-2948/2013/0507>
- Amézquita, A., Lima, A. P., Jehle, R., Castellanos, L., Ramos, Ó., Crawford, A. J., ... Hödl, W. (2009). Calls, colours, shape, and genes: A multi-trait approach to the study of geographic variation in the Amazonian frog *Allobates femoralis*. *Biological Journal of the Linnean Society*, 98, 826–838. <https://doi.org/10.1111/j.1095-8312.2009.01324.x>

- Bioacoustics Research Program. (2015). *Raven Pro: Interactive Sound Analysis Software*. Ver. 1.5. Ithaca, NY: The Cornell Lab of Ornithology. Available from <http://www.birds.cornell.edu/raven>
- Blaustein, A. R., Kiesecker, J. M., Chivers, D. P., & Anthony, R. G. (1997). Ambient UV-B radiation causes deformities in amphibian embryos. *Proceedings of the National Academy of Sciences*, *94*(25), 13735–13737. <https://doi.org/10.1073/pnas.94.25.13735>
- Caldwell, J. P., & Lima, A. P. (2003). A new Amazonian species of *Colostethus* (Anura: Dendrobatidae) with a nidicolous tadpole. *Herpetologica*, *59*, 219–234. [https://doi.org/10.1655/0018-0831\(2003\)059\[0219:ANASOC\]2.0.CO;2](https://doi.org/10.1655/0018-0831(2003)059[0219:ANASOC]2.0.CO;2)
- Caldwell, J. P., Lima, A. P., & Keller, C. (2002). Redescription of *Colostethus marchesianus* (Melin, 1941) from its type locality. *Copeia*, *2002*, 157–165. [https://doi.org/10.1643/0045-8511\(2002\)002\[0157:ROCMMF\]2.0.CO;2](https://doi.org/10.1643/0045-8511(2002)002[0157:ROCMMF]2.0.CO;2)
- Caminer, M. A., Milá, B., Jansen, M., Fouquet, A., Venegas, P. J., Chávez, G., ... Ron, S. R. (2017). Systematics of the *Dendropsophus leucophyllatus* species complex (Anura: Hylidae): Cryptic diversity and the description of two new species. *PLoS One*, *12*, e0171785. <https://doi.org/10.1371/journal.pone.0171785>
- Caminer, M. A., & Ron, S. R. (2014). Systematics of treefrogs of the *Hypsiboas calcaratus* and *Hypsiboas fasciatus* species complex (Anura: Hylidae) with the description of four new species. *ZooKeys*, *370*, 1–68. <https://doi.org/10.3897/zookeys.370.6291>
- Cintra, B. B. L., Schiatti, J., Emillio, T., Martins, D., Moulatlet, G., Souza, P., ... Schöngart, J. (2013). Soil physical restrictions and hydrology regulate stand age and wood biomass turnover rates of Purus-Madeira interfluvial wetlands in Amazonia. *Biogeosciences*, *10*, 7759–7774. <https://doi.org/10.5194/bg-10-7759-2013>
- Clough, M., & Summers, K. (2000). Phylogenetic systematics and biogeography of the poison frogs: Evidence from mitochondrial DNA sequences. *Biological Journal of the Linnean Society*, *70*, 515–540. <https://doi.org/10.1111/j.1095-8312.2000.tb01236.x>
- Core Team, R. (2017). *R: A language and environment for statistical computing*. Vienna, Austria: R Foundation for Statistical Computing. Retrieved from: <https://www.R-project.org/>
- Dias-Terceiro, R. G., Kaefer, I. L., Fraga, R., Araújo, M. C., Simões, P. I., & Lima, A. P. (2015). A matter of scale: Historical and environmental factors structure anuran assemblages from the upper madeira river, Amazonia. *Biotropica*, *47*, 259–266. <https://doi.org/10.1111/btp.12197>
- Fearnside, P. M., & Graça, P. M. L. A. (2006). BR-319: Brazil's Manaus-Porto Velho Highway and the potential impact of linking the arc of deforestation to central Amazonia. *Environmental Management*, *38*(5), 705–716. <https://doi.org/10.1007/s00267-005-0295-y>
- Ferrão, M., Colatreli, O., Fraga, R., Kaefer, I. L., Moravec, J., & Lima, A. P. (2016). High species richness of *Scinax* treefrogs (Hylidae) in a threatened Amazonian landscape revealed by an integrative approach. *PLoS One*, *11*, e0165-679. <https://doi.org/10.1371/journal.pone.0165679>
- Ferrão, M., Moravec, J., Fraga, R., Almeida, A. P., Kaefer, I. L., & Lima, A. P. (2017). A new species of *Scinax* from the Purus-Madeira interfluvium. Brazilian Amazonia (Anura, Hylidae). *ZooKeys*, *706*, 137–162. <https://doi.org/10.3897/zookeys.706.14691>
- Ferreira, A. S., Jehle, R., Stow, A. J., & Lima, A. P. (2018). Soil and forest structure predict large-scale patterns of occurrence and local abundance of a widespread Amazonian frog. *PeerJ*, *6*, e5424. <https://doi.org/10.7717/peerj.5424>
- Fouquet, A., Cassini, C. S., Haddad, C. F. B., Pech, N., & Rodrigues, M. T. (2013). Species delimitation, patterns of diversification and historical biogeography of the Neotropical frog genus *Adenomera* (Anura: Leptodactylidae). *Journal of Biogeography*, *41*, 855–870. <https://doi.org/10.1111/jbi.12250>
- Fouquet, A., Gilles, A., Vences, M., Marty, C., Blanc, M., & Gemmill, N. J. (2007). Underestimation of species richness in neotropical frogs revealed by mtDNA analyses. *PLoS One*, *2*(10), e1109. <https://doi.org/10.1371/journal.pone.0001109>
- Fouquet, A., Loebmann, D., Castroviejo-Fisher, S., Padial, J. M., Orrico, V. G. D., Lyra, M. L., & Rodrigues, M. T. (2012). From Amazonia to the Atlantic forest: Molecular phylogeny of Phyzelaphryninae frogs reveals unexpected diversity and a striking biogeographic pattern emphasizing conservation challenges. *Molecular Phylogenetics and Evolution*, *65*(2), 547–561. <https://doi.org/10.1016/j.ympev.2012.07.012>
- Frost, D. R. (2019, December 30). *Amphibian Species of the World: An Online Reference (Version 6.0)*. Retrieved from: <http://research.amnh.org/herpetology/amphibia/index.html>
- Funk, W. C., Caminer, M., & Ron, S. R. (2012). High levels of cryptic species diversity uncovered in Amazonian frogs. *Proceedings Biological Sciences*, *279*(1734), 1806–1814. <https://doi.org/10.1098/rspb.2011.1653>
- Glaw, F., & Vences, M. (2006). Phylogeny and genus-level classification of mantellid frogs (Amphibia, Anura). *Organisms Diversity & Evolution*, *6*(3), 236–253. <https://doi.org/10.1016/j.ode.2005.12.001>
- Gosner, K. L. (1960). A simplified table for staging anuran embryos and larvae with notes on identification. *Herpetologica*, *16*(3), 183–190. <https://www.jstor.org/stable/3890061>
- Grant, T., Frost, D. R., Caldwell, J. P., Gagliardo, R., Haddad, C. F. B., Kok, P. J. R., ... Wheeler, W. C. (2006). Phylogenetic systematics of dart-poison frogs and their relatives (Anura: Athesphatanura: Dendrobatidae). *Bulletin of the American Museum of Natural History*, *299*, 1–262. [https://doi.org/10.1206/0003-0090\(2006\)299\[1:P-SODFA\]2.0.CO;2](https://doi.org/10.1206/0003-0090(2006)299[1:P-SODFA]2.0.CO;2)
- Grant, T., Rada, M., Anganoy-Criollo, M., Batista, A., Dias, P. H., Jeckel, A. M., ... Rueda-Almonacid, J. V. (2017). Phylogenetic systematics of dart-poison frogs and their relatives revisited (Anura: Dendrobatoidea). *South American Journal of Herpetology*, *12*, 1–90. <https://doi.org/10.2994/SAJH-D-17-00017.1>
- Guarnizo, C. E., Paz, A., Muñoz-Ortiz, A., Flechas, S. V., Méndez-Narváez, J., & Crawford, A. J. (2015). DNA barcoding survey of anurans across the eastern cordillera of Colombia and the impact of the Andes on cryptic diversity. *PLoS One*, *10*(5), e0127312. <https://doi.org/10.1371/journal.pone.0127312>
- Guindon, S., Dufayard, J. F., Lefort, V., Anisimova, M., Hordijk, W., & Gascuel, O. (2010). New algorithms and methods to estimate maximum likelihood phylogenies: Assessing the performance of PhyML 3.0. *Systematic Biology*, *59*, 307–321. <https://doi.org/10.1093/sysbio/syq010>
- Gurdon, J. B. (1960). The effects of ultraviolet irradiation on uncleaved eggs of *Xenopus laevis*. *Quarterly Journal of Microscopical Sciences*, *101*, 299–311.
- Hall, T. A. (1999). BioEdit: A user-friendly biological sequence alignment editor and analysis program for Windows 95/98/NT. *Nucleic Acids Symposium Series*, *41*, 95–98.
- IBGE - Instituto Brasileiro de Geografia e Estatística. (2012). *Manual técnico da vegetação brasileira: Sistema fitogeográfico, inventário das formações florestais e campestres, técnicas e manejo de coleções botânicas, procedimentos para mapeamentos*, 2nd ed. Rio de Janeiro, RJ: IBGE- Diretoria de Geociências.
- Jombart, T., & Ahmed, I. (2011). ADEGENET 1.3-1: New tools for the analysis of genome-wide SNP data. *Bioinformatics*, *27*(21), 3070–3071. <https://doi.org/10.1093/bioinformatics/btr521>
- Jombart, T., Devillard, S., & Balloux, F. (2010). Discriminant analysis of principal components: A new method for the analysis of genetically structured populations. *BMC Genetics*, *11*(1), 94. <https://doi.org/10.1186/1471-2156-11-94>
- Kaefer, I. L., Tsuji-Nishikido, B. M., & Lima, A. P. (2012). Beyond the river: Underlying determinants of population acoustic signal variability in Amazonian direct-developing *Allobates* (Anura: Dendrobatoidea). *Acta Ethologica*, *15*, 187–194. <https://doi.org/10.1007/s10211-012-0126-0>

- Kearse, M., Moir, R., Wilson, A., Stones-Havas, S., Cheung, M., Sturrock, S., ... Drummond, A. (2012). Geneious Basic: An integrated and extendable desktop software platform for the organization and analysis of sequence data. *Bioinformatics*, 28, 1647–1649. <https://doi.org/10.1093/bioinformatics/bts199>
- Kimura, M. (1980). A simple method for estimating evolutionary rates of base substitutions through comparative studies of nucleotide sequences. *Journal of Molecular Evolution*, 16, 111–120. <https://doi.org/10.1007/bf01731581>
- Kusano, T., Maruyama, K., & Kanenko, S. (1999). Breeding site fidelity in the Japanese toad, *Bufo japonicus formosus*. *Herpetological Journal*, 9, 9–13.
- La Marca, E., Vences, M., & Lötters, S. (2002). Rediscovery and mitochondrial relationships of the dendrobatid frog *Colostethus humilis* suggest parallel colonization of the Venezuelan Andes by poison frogs. *Studies on Neotropical Fauna and Environment*, 37, 233–240. <https://doi.org/10.1076/snfe.37.3.233.8566>
- Lanfear, R., Frandsen, P. B., Wright, A. M., Senfeld, T., & Calcott, B. (2016). PartitionFinder 2: New methods for selecting partitioned models of evolution for molecular and morphological phylogenetic analyses. *Molecular Biology and Evolution*, 34, 772–773. <https://doi.org/10.1093/molbev/msw260>
- Liaw, A., & Wiener, M. (2002). Classification and regression by RandomForest. *R News*, 2(3), 18–22.
- Lima, A. P., & Caldwell, J. P. (2001). A new Amazonian species of *Colostethus* with sky blue digits. *Herpetologica*, 57, 133–138.
- Lima, A. P., Caldwell, J. P., Biavati, G., & Montanarin, A. (2010). A new species of *Allobates* (Anura: Aromobatidae) from Paleovárzea Forest in Amazonas, Brazil. *Zootaxa*, 2337, 1–17. <https://doi.org/10.11646/zootaxa.2337.1.1>
- Lima, A. P., Caldwell, J. P., & Strüssmann, C. (2009). Redescription of *Allobates brunneus* (Cope) 1887 (Anura: Aromobatidae: Allobatinae), with a description of the tadpole, call, and reproductive behavior. *Zootaxa*, 1988, 1–16. <https://doi.org/10.11646/zootaxa.1988.1.1>
- Lima, A. P., Erdtmann, L. K., & Amézquita, A. (2012). Advertisement call and colour in life of *Allobates crombiei* (Morales) “2000” [2002] (Anura: Aromobatidae) from the type locality (Cachoeira do Espelho), Xingu River, Brazil. *Zootaxa*, 3475, 86–88. <https://doi.org/10.11646/zootaxa.3475.1.8>
- Lima, A. P., Sanchez, D. E. A., & Souza, J. R. D. (2007). A new Amazonian species of the frog genus *Colostethus* (Dendrobatidae) that lays its eggs on undersides of leaves. *Copeia*, 2007, 114–122. [https://doi.org/10.1643/0045-8511\(2007\)7\[114:ANASOT\]2.0.CO;2](https://doi.org/10.1643/0045-8511(2007)7[114:ANASOT]2.0.CO;2)
- Lima, A. P., Simões, P. I., & Kaefer, I. L. (2014). A new species of *Allobates* (Anura: Aromobatidae) from the Tapajós River basin, Pará State, Brazil. *Zootaxa*, 3889, 355–387. <https://doi.org/10.11646/zootaxa.3889.3.2>
- Lima, A. P., Simões, P. I., & Kaefer, I. L. (2015). A new species of *Allobates* (Anura: Aromobatidae) from Parque Nacional da Amazônia, Pará State, Brazil. *Zootaxa*, 3980, 501–525. <https://doi.org/10.11646/zootaxa.3980.4.3>
- Maddison, W. P., & Maddison, D. R. (2015). *Mesquite: A Modular System for Evolutionary Analysis. Version 3.04*. Retrieved from: <http://mesquiteproject.org>
- Magnusson, W. E., Braga-Neto, R., Pezzini, F., Baccaro, F., Bergallo, H., Penha, J., ... Pontes, A. R. M. (2013). *Biodiversidade e monitoramento ambiental integrado: O sistema RAPELD na Amazônia*. Santo André: Attema.
- Maia, G. F., Lima, A. P., & Kaefer, I. L. (2017). Not just the river: Genes, shapes, and sounds reveal population-structured diversification in the Amazonian frog *Allobates tapajos* (Dendrobatoidea). *Biological Journal of the Linnean Society*, 121(1), 95–108. <https://doi.org/10.1093/biolinnean/blw017>
- Melo-Sampaio, P. R., Oliveira, R. M., & Prates, I. (2018). A new Nurse Frog from Brazil (Aromobatidae: *Allobates*). with data on the distribution and phenotypic variation of western Amazonian species. *South American Journal of Herpetology*, 13, 131–149. <https://doi.org/10.2994/SAJH-D-17-00098.1>
- Melo-Sampaio, P. R., Souza, M. B., & Peloso, P. L. V. (2013). A new riparian species of *Allobates* Zimmermann and Zimmermann, 1988 (Anura: Aromobatidae) from southwestern Amazonia. *Zootaxa*, 3716(3), 336–348. <https://doi.org/10.11646/zootaxa.3716.3.2>
- Miller, M. A., Pfeiffer, W., & Schwartz, T. (2010). Creating the CIPRES Science Gateway for inference of large phylogenetic trees. In *Proceedings of the Gateway Computing Environments Workshop*. New Orleans, LA.
- Moraes, L. J. C. L., Pavan, D., & Lima, A. P. (2019). A new nurse frog of *Allobates masniger-nidicola* complex (Anura, Aromobatidae) from the east bank of Tapajós River, eastern Amazonia. *Zootaxa*, 4648(3), 401–434. <https://doi.org/10.11646/zootaxa.4648.3.1>
- Myers, C. W., Paolillo-O, A., and Daly, J. W. (1991). Discovery of a defensively malodorous and nocturnal frog in the family Dendrobatidae: Phylogenetic significance of a new genus and species from Venezuelan Andes. *American Museum Novitates*, 3002, 1–33.
- Ohler, A., & Dubois, A. (2006). Phylogenetic relationships and generic taxonomy of the tribe Paini (Amphibia, Anura, Ranidae, Dicroglossinae) with diagnoses of two new genera. *Zoosystema*, 28, 769–784.
- Ortiz, D. A., Lima, A. P., & Werneck, F. P. (2018). Environmental transition zone and rivers shape intraspecific population structure and genetic diversity of an Amazonian rain forest tree frog. *Evolutionary Ecology*, 32(4), 359–378. <https://doi.org/10.1007/s10682-018-9939-2>
- Ovaska, K. (1992). Short- and long-term movements of the frog *Eleuterodactylus johnstonei* in Barbados, West Indies. *Copeia*, 1992, 569–573. <https://doi.org/10.2307/1446223>
- Padial, J. M., & De la Riva, I. (2009). Integrative taxonomy reveals cryptic Amazonian species of *Pristimantis* (Anura: Strabomantidae). *Zoological Journal of the Linnean Society*, 155, 97–122. <https://doi.org/10.1111/j.1096-3642.2008.00424.x>
- Palumbi, S. R. (1996). Nucleic acids II: The polymerase chain reaction. In D. M. Hillis, C. Moritz, & B. K. Mable (Eds.), *Molecular systematics* (pp. 205–247). Sunderland, MA: Sinauer & Associates.
- Pinheiro, P. D. P., Kok, P. J. R., Noonan, B. P., Means, D. B., Haddad, C. F. B., & Faivovich, J. (2019). A new genus of Cophomantini, with comments on the taxonomic status of *Boana lilliae* (Anura: Hylidae). *Zoological Journal of the Linnean Society*, 185, 226–245. <https://doi.org/10.1093/zoolinnean/zly030>
- Rambaut, A., Drummond, A. J., Xie, D., Baele, G., & Suchard, M. A. (2018). Posterior summarization in Bayesian phylogenetics using Tracer 1.7. *Systematic Biology*, 67(5), 901–904. <https://doi.org/10.1093/sysbio/syy032>
- Ringler, M., Ursprung, E., & Hödl, W. (2009). Site fidelity and patterns of short- and long-term movement in the brilliant-thighed poison frog *Allobates femoralis* (Aromobatidae). *Behavioral Ecology and Sociobiology*, 63(6), 1281–1293. <https://doi.org/10.1007/s00265-009-0793-7>
- Rivadeneira, C. D., Venegas, P. J., & Ron, S. R. (2018). Species limits within the widespread Amazonian treefrog *Dendropsophus parviceps* with descriptions of two new species (Anura, Hylidae). *ZooKeys*, 726, 25–77. <https://doi.org/10.3897/zookeys.726.13864>
- Rocha, S. M. C., Lima, A. P., & Kaefer, I. L. (2018). Territory size as a main driver of male-mating success in an Amazonian nurse frog (*Allobates paleovarzensis*, Dendrobatoidea). *Acta Ethologica*, 21, 51–57. <https://doi.org/10.1007/s10211-017-0280-5>
- Rojas, R. R., Fouquet, A., Ron, S. R., Hernández-Ruz, E. J., Melo-Sampaio, P. R., Chaparro, J. C., ... Hrbek, T. (2018). A Pan-Amazonian species delimitation: High species diversity within the genus *Amazophrynella* (Anura: Bufonidae). *PeerJ*, 6, e4941. <https://doi.org/10.7717/peerj.4941>
- Ronquist, F., Teslenko, M., Van Der Mark, P., Ayres, D. L., Darling, A., Höhna, S., ... Huelsenbeck, J. P. (2012). MrBayes 3.2: Efficient

- Bayesian phylogenetic inference and model choice across a large model space. *Systematic Biology*, 61, 539–542. <https://doi.org/10.1093/sysbio/sys029>
- Sá, R. O., Grant, T., Camargo, A., Heyer, W. R., Ponsa, M. L., & Stanley, E. (2014). Systematics of the neotropical genus *Leptodactylus* Fitzinger, 1826 (Anura: Leptodactylidae): Phylogeny, the relevance of non-molecular evidence, and species accounts. *South American Journal of Herpetology*, 9, S1–S100. <https://doi.org/10.2994/SAJH-D-13-00022.1>
- Santos, J. C., Coloma, L. A., Summers, K., Caldwell, J. P., Ree, R., & Cannatella, D. C. (2009). Amazonian amphibian diversity is primarily derived from late Miocene Andean lineages. *PLoS Biology*, 7, 448–461. <https://doi.org/10.1371/journal.pbio.1000056>
- Schiatti, J., Martins, D., Emilio, T., Souza, P. F., Levis, C., Baccaro, F. B., ... Magnusson, W. E. (2016). Forest structure along a 600 km transect of natural disturbances and seasonality gradients in central-southern Amazonia. *Journal of Ecology*, 104, 1335–1346. <https://doi.org/10.1111/1365-2745.12596>
- Schulze, A., Jansen, M., & Köhler, G. (2015). Tadpole diversity of Bolivia's lowland anuran communities: Molecular identification, morphological characterization, and ecological assignment. *Zootaxa*, 4016(1), 1–111. <https://doi.org/10.11646/zootaxa.4016.1.1>
- Simões, P. I. (2016). A new species of nurse-frog (Aromobatidae) from the Madeira River basin with a small geographic range. *Zootaxa*, 4083, 501–525. <https://doi.org/10.11646/zootaxa.4083.4.3>
- Simões, P. I., Gagliardi-Urrutia, L. A. G., Rojas-Runjaic, F. J. M., & Castroviejo-Fisher, S. (2018). A new species of nurse-frog (Aromobatidae. *Allobates*) from the Juami River basin. north-western Brazilian Amazonia. *Zootaxa*, 4387, 109–133. <https://doi.org/10.11646/zootaxa.4387.1.5>
- Simões, P. I., Lima, A. P., & Farias, I. P. (2010). The description of a cryptic species related to the pan-Amazonian frog *Allobates femoralis* (Boulenger, 1883) (Anura: Aromobatidae). *Zootaxa*, 2406, 1–28. <https://doi.org/10.11646/zootaxa.2406.1.1>
- Simões, P. I., Lima, A. P., Magnusson, W. E., Hödl, W., & Amézquita, A. (2008). Acoustic and Morphological Differentiation in the Frog *Allobates femoralis*: Relationships with the Upper Madeira River and Other Potential Geological Barriers. *Biotropica*, 40, 607–614. <https://doi.org/10.1111/j.1744-7429.2008.00416.x>
- Simões, P. I., Rojas, D., & Lima, A. P. (2019). A name for the nurse-frog (*Allobates*, Aromobatidae) of Floresta Nacional de Carajás, Eastern Brazilian Amazonia. *Zootaxa*, 4550, 71–100. <https://doi.org/10.11646/zootaxa.4550.1.3>
- Simões, P. I., Sturaro, M. J., Peloso, P. L. V., & Lima, A. P. (2013). A new diminutive species of *Allobates* Zimmermann and Zimmermann, 1988 (Anura. Aromobatidae) from the northwestern Rio Madeira/Rio Tapajós interfluvio, Amazonas, Brazil. *Zootaxa*, 3609, 251–273. <https://doi.org/10.11646/zootaxa.3609.3.1>
- Tamura, K., Stecher, G., Peterson, D., Filipski, A., & Kumar, S. (2013). MEGA6: Molecular evolutionary genetics analysis version 6.0. *Molecular Biology and Evolution*, 30, 2725–2729. <https://doi.org/10.1093/molbev/mst197>
- Thompson, J. D., Higgins, D. G., & Gibson, T. J. (1994). Clustal W: Improving the sensitivity of progressive multiple sequence alignment through sequence weighting, position-specific gap penalties and weight matrix choice. *Nucleic Acids Research*, 22(22), 4673–4680. <https://doi.org/10.1093/nar/22.22.4673>
- Toledo, L. F., & Batista, R. F. (2012). Integrative study of Brazilian Anurans: Geographic distribution, size, environment, taxonomy, and conservation. *Biotropica*, 44, 785–792. <https://doi.org/10.1111/j.1744-7429.2012.00866.x>
- Tsuji-Nishikido, B. M., Kaefer, I. L., Freitas, F. C., Menin, M., & Lima, A. P. (2012). Significant but not diagnostic: Differentiation through morphology and calls in the Amazonian frogs *Allobates nidicola* and *A. masniger*. *Herpetological Journal*, 22, 105–114.
- Zhang, J., Kapli, P., Pavlidis, P., & Stamatakis, A. (2013). A general species delimitation method with applications to phylogenetic placements. *Bioinformatics*, 29, 2869–2876. <https://doi.org/10.1093/bioinformatics/btt499>

## SUPPORTING INFORMATION

Additional supporting information may be found online in the Supporting Information section at the end of the article.

**Figure S1.** Phylogeny of the *Allobates* based on four mitochondrial (12S, 16S, COI, CYTB) and six nuclear genes (28S, HH3, RAG1, RHO, SINA, TYR).

**Alignment S1.** Alignment of four mitochondrial (12S, 16S, COI, CYTB) and six nuclear genes (28S, HH3, RAG1, RHO, SINA, TYR) consisting of 5,914 base pairs and 93 taxa used in phylogenetic analyses.

**Table S1.** Species, vouchers and GenBank accession numbers of samples used in phylogenetic analyses. Bold accession numbers represent the specimens sequenced in the present study. Abbreviations: Ref. = references, s.s. = sensu stricto; s.l. = sensu lato.

**Table S2.** Species, vouchers and localities of samples used in phylogenetic analyses.

**Table S3.** Selected partitions and evolutionary models proposed by Bayesian Inference Criterion through PhyML algorithm as implemented in PartitionFinder. Numbers after gene name denote the codon position. PT = partitions.

**Table S4.** DAPC group memberships of 68 males of *Allobates tinae* sensu lato based on 23 morphometric measurements. INPAH = Herpetological collection of the Instituto Nacional de Pesquisas da Amazônia.

**Table S5.** DAPC group memberships of 17 males of *Allobates tinae* sensu lato based on 16 bioacoustic measurements. Abbreviations: INPAH = Herpetological collection of the Instituto Nacional de Pesquisas da Amazônia; CENBAM = Bioacoustic repository of the Centro de Estudos Integrados da Biodiversidade Amazônica at INPA, Manaus, Brazil.

**How to cite this article:** Lima AP, Ferrão M, Lacerda da Silva D. Not as widespread as thought: Integrative taxonomy reveals cryptic diversity in the Amazonian nurse frog *Allobates tinae* Melo-Sampaio, Oliveira and Prates, 2018 and description of a new species. *J Zool Syst Evol Res*. 2020;58:1173–1194. <https://doi.org/10.1111/jzs.12406>

## APPENDIX 1

## —Specimens examined.

***Allobates bacurau***

Adults. BRAZIL: AMAZONAS: Estrada do Miriti, Manicoré [INPAH 35398 (holotype); 35397, 35399–35409 (paratypes)].

***Allobates caeruleodactylus***

Adults. BRAZIL: AMAZONAS: km 12 on the road to Autazes [INPAH 7238 (holotype); 7229–7232, 7234–7237 (paratypes)]. Tadpoles. BRAZIL: AMAZONAS: km 12 on the road to Autazes (INPAH 8037–8046, INPA- H 8085).

***Allobates crombiei***

Adults. BRAZIL: PARÁ: Cachoeira do Espelho [INPAH 30457–30477 (topotypes)].

***Allobates fuscillus***

Adults. BRAZIL: AMAZONAS: Ipixuna: Penedo, east bank of Juruá river [INPAH 2532 (holotype); 2531 (paratopotype)]; Itamarati: Jainu, Juruá River [INPAH 3114, 3250, 3270, 3514 (paratypes)].

***Allobates gasconi***

Adults. BRAZIL: AMAZONAS: Itamarati: Jainu, west bank of Juruá River [INPAH 3082 (holotype); 3073, 3079, 3085, 3090, 3150, 3151, 3172, 3249, 3406, 3415, 3483, 3484, 3491, 3494, 3496, 3512, 3513 (paratypes)].

***Allobates grillisimilis***

Adults. BRAZIL: AMAZONAS: Borba [INPAH 30779 (holotype); 30780–30808 (paratopotypes)]; Nova Olinda do Norte [INPAH 30809–30823 (paratypes)].

***Allobates magnussoni***

Adults. BRAZIL: PARÁ: Parque Nacional da Amazônia [INPAH 32960 (holotype); 32961–32976, 32978–32982 (paratopotypes)]; Treviso (INPAH 10105–10109, 33930–33934). Tadpoles. BRAZIL: PARÁ: Treviso (INPAH 10054, 10056, 10058, 10059, 10060).

***Allobates marchesianus***

Adults. BRAZIL: AMAZONAS: Missão Taracú [INPAH 7959–7990 (topotypes)]; São Gabriel da Cachoeira, 175 km E Missão Taracú (INPAH 7991, 7993, 8000–8007). Tadpoles. BRAZIL: AMAZONAS: Missão Taracú [INPAH 7943–7950, 7992, 7998, 8084 (topotypes)].

***Allobates masniger***

Adults. BRAZIL: AMAZONAS: Borba (INPAH 28075, 28078, 28084, 28089, 28092, 28095, 28098, 28100, 28104, 28105, 28112, 28114,

28119); PARÁ: Parque Nacional da Amazônia [INPAH 28195–28217 (topotypes)]; Jacareacanga (INPAH 28053, 28070, 28077, 28082, 28093, 28094, 28099, 28103, 28107, 28110, 28111, 28113, 28115, 28118, 28120).

***Allobates nidicola***

Adults. BRAZIL: AMAZONAS: km 12 on road to Autazes [INPAH 8093 (holotype); 7253–7259, 7261, 7262, 8094 (paratypes); INPAH 28122, 28124, 28127, 28129, 28131, 28144, 28159, 28163, 28166, 28169, 28171, 28172, 28174, 28179, 28184, 28185 (topotypes)]. Tadpoles. BRAZIL: AMAZONAS: km 12 on road to Autazes (INPAH 8021–8033, 8137–8139).

***Allobates nunciatus***

Adults. BRAZIL: PARÁ: Itaituba [INPAH 40486 (holotype); 40305, 40307, 40475, 40480, 40485, 40489, 40324, 40476 (paratypes); Trairão [INPA-H 40482, 40484, 40488 (paratypes)].

***Allobates paleovarzensis***

Adults. BRAZIL: AMAZONAS: Careiro da Várzea [INPAH 20904 (holotype); 20861–20903, 20905 (paratypes)].

***Allobates subfolionidificans***

Adults. BRAZIL: ACRE: Parque Zoobotânico da Universidade Federal do Acre [INPAH 13760 (holotype); 11958–11974, 13749–13754, 13756–13759, 13761, 13762 (paratypes)]. Tadpoles. BRAZIL: ACRE: Parque Zoobotânico da Universidade Federal do Acre (INPAH 14822, 14823).

***Allobates tapajos***

Adults. BRAZIL: PARÁ: Parque Nacional da Amazônia [INPAH 34425 (holotype); 34402–34424 (paratypes)]. Tadpoles. BRAZIL: PARÁ: Parque Nacional da Amazônia (Lots INPAH 34426, 34427).

***Allobates trilineatus***

Adults. BRAZIL: ACRE: Parque Zoobotânico da Universidade Federal do Acre (INPAH 11958–11993).

***Allobates vanzolinus***

Adults. BRAZIL: AMAZONAS: Vai-Quem-Quer, Rio Juruá [INPAH 4896 (holotype); 4903, 4904, 4905, 4912 (paratypes)]; Jainu, Rio Juruá [INPAH 3381, 3413 (paratypes)].